Palaeogeography, Palaeoclimatology, Palaeoecology 618 (2023) 111496

Contents lists available at ScienceDirect

Palaeogeography, Palaeoclimatology, Palaeoecology

journal homepage: www.elsevier.com/locate/palaeo

Redox conditions and ecological resilience during Oceanic Anoxic Event 2 in the Western Interior Seaway

L.J. Robinson [a,*], K.S. George [a], C.P. Fox [b], J.E.A. Marshall [a], I.C. Harding [a], P.R. Bown [c], J.R. Lively [d], S. Marroquín [e], R.M. Leckie [f], S. Dameron [f], D.R. Gröcke [g], N.M. Papadomanolaki [h,1], N.A.G.M. van Helmond [h], J.H. Whiteside [a,i]

[a] School of Ocean and Earth Science, University of Southampton, National Oceanography Centre, Southampton, SO14 3ZH, UK
[b] Department of Earth Science, Khalifa University of Science and Technology, Abu Dhabi, United Arab Emirates
[c] Department of Earth Science, University College London, UK
[d] Prehistoric Museum, Utah State University Eastern, Price, UT, USA
[e] Division of Geological and Planetary Sciences, California Institute of Technology, Pasadena, CA, USA
[f] Department of Geosciences, University of Massachusetts, Amherst, USA
[g] Department of Earth Sciences, Durham University, Durham DH1 3LE, UK
[h] Department of Earth Sciences, Utrecht University, Utrecht, the Netherlands
[i] Department of Geological Sciences, San Diego State University, 5500 Campanile Dr, San Diego, CA 92182, USA

ARTICLE INFO

Editor: Dr. A Dickson

Original content: Robinson et al C/T organic geochem data from five sites in the Western Interior Seaway (Original data)

Keywords:
Cretaceous
Prasinophytes
Steranes
Organic geochemistry

ABSTRACT

Oceanic Anoxic Events (OAEs) are important geological events that may be analogues to future climate-driven deoxygenation of our oceans. Much of the global ocean experienced anoxic conditions during the Cenomanian–Turonian OAE (OAE2; ~94 Ma), whereas the Western Interior Seaway (WIS) experienced oxygenation at this time. Here, organic geochemical and palynological data generated from Cenomanian–Turonian age sediments from five sites in the WIS are used to investigate changing redox and ecological conditions across differing palaeoenvironments and palaeolatitudes. Heterogeneity across the sites is apparent, but important relationships and trends among oceanographic variables are recognised: 1) Increasing total organic carbon (TOC) and $CaCO_3$ percentages indicate the onset of a sea-level maximum towards the end of OAE2; 2) C_{28} sterane is shown to be a useful marker for prasinophyte abundance, and concurrent increases in this marker and overall sterane abundance indicate prasinophyte-driven increase in algal productivity in a stratified water column; and 3) sterane ratios can be a more reliable geochemical proxy than redox proxies for assessing the Benthic Oxic Zone. Our redox data do not always follow established trends for the WIS overall, particularly for proximal settings. We therefore surmise that local effects, such as nutrient-driven expansion of the oxygen minimum zone and/or sedimentation-driven anoxia just below the sediment-water interface, have overprinted regional trends.

1. Introduction

Oceanic Anoxic Events (OAEs) are acute events of <1 million years duration associated with episodes of rapid climatic warming, widespread marine deoxygenation, perturbations of a variety of biogeochemical cycles, deposition of organic-rich sediments and biotic turnovers (Schlanger and Jenkyns, 1976; Leckie et al., 2002; Jenkyns, 2010; Robinson et al., 2017). Although OAEs have been recognised as predominantly occurring in the Mesozoic Era (~252–66 Ma), similar environmental changes are being reported in our currently rapidly changing climate (IPCC, 2021). Elevated modern global temperatures (Hawkins et al., 2017), coupled with decreasing oxygen content in the modern ocean (Keeling et al., 2010; Schmidtko et al., 2017; Breitburg et al., 2018) and indications of species loss (Barnosky et al., 2011; Dirzo et al., 2014; Ceballos et al., 2017) suggest that a better understanding of past environmental trends during OAEs can provide key insights into the trajectory of global climate in the coming decades and beyond.

The mid-Cretaceous Oceanic Anoxic Event 2 (OAE2; ~94 Ma) occurred during the Cenomanian–Turonian (C–T) thermal maximum (Jenkyns, 1980; O'Brien et al., 2017), and is thought to have been

* Corresponding author.
E-mail address: ejr1n17@soton.ac.uk (L.J. Robinson).
[1] Now at: Aix Marseille University, CNRS, IRD, Coll France, INRA, CEREGE, Aix en Provence, France

https://doi.org/10.1016/j.palaeo.2023.111496
Received 10 August 2022; Received in revised form 3 March 2023; Accepted 5 March 2023
Available online 8 March 2023

triggered by large-scale volcanism that injected CO_2, sulfides and trace metals into the ocean and atmosphere (Kuroda et al., 2007; Turgeon and Creaser, 2008; Jarvis et al., 2011; Du Vivier et al., 2014). The ensuing increases in temperature resulted in: (1) sluggish oceanic circulation (Erbacher et al., 2001; Kidder and Worsley, 2010); (2) a strengthened hydrological cycle, promoting continental run-off and nutrient addition to the oceans (Arthur et al., 1987; Adams et al., 2010; Trabucho Alexandre et al., 2010; Monteiro et al., 2012; van Helmond et al., 2014); and (3) transgression in shallow epicontinental seas (Arthur and Sageman, 2005). Primary productivity flourished under these conditions, culminating in widespread algal productivity, anoxic bottom waters, higher rates of organic carbon burial and a globally recognised positive carbon isotope excursion (CIE) (Jenkyns, 2003, 2010; Robinson et al., 2017).

Organic matter produced during OAE2 is preserved globally (Schlanger et al., 1987; Takashima et al., 2006; Robinson et al., 2017). It is estimated that 40–50% of the world's ocean by volume could have experienced anoxic conditions (Monteiro et al., 2012; Ostrander et al., 2017), with 2–5% of the world's ocean becoming euxinic (Owens et al., 2013; Dickson et al., 2016a, 2016b). However, unlike the globally synchronous CIE, deposition of organic matter varied spatially (Vizcaíno et al., 2020) and in some cases was diachronous within basins (Tsikos et al., 2004).

The Western Interior Seaway (WIS) of North America is enigmatic in that it does not conform to global trends of deoxygenation and organic enrichment during OAE2 (Vizcaíno et al., 2020). Whilst anoxia and deposition of organic matter was increasing across the world, the WIS experienced intervals of oxygenation and lower organic enrichment during OAE2. Here, we present an extensive, high-resolution organic geochemical and palynological study across a depth-transect spanning 21° of palaeolatitude through the WIS to determine the extent of anoxia, its drivers, and associated ecological reorganization before, during and after OAE2.

1.1. Geological background

The WIS was a shallow epicontinental seaway comprised of a rapidly subsiding clastic-rich foredeep, discrete zones of forebulge uplift, a wider more moderately subsiding central axial basin and a stable, broad cratonic platform to the east (Fig. 1; Arthur and Sageman, 2005; Kauffman, 1984). Marine inputs to the basin originated from both northern Boreal and southern Tethyan ocean sources, whose relative contributions varied over time. As a relatively shallow and restricted basin the WIS regularly experienced low oxygen conditions and organic enrichment throughout the Cretaceous, however several studies have shown oxygenation of the water column and a pause in organic enrichment in the central WIS during the initial onset of OAE2 (Eicher and Diner, 1985; Leckie et al., 1998; Savrda, 1998; Elderbak et al., 2014; Eldrett et al., 2014; Lowery et al., 2017, 2018).

The expression of this oxygenation event in WIS sediments is sometimes termed the Benthonic Zone (BOZ: Eicher and Worstell, 1970), characterised by a decrease in total organic carbon (TOC) and redox-sensitive trace metal concentrations, concurrent with an increase in diversity and abundance of faunal assemblages and increased bioturbation (Eicher and Worstell, 1970; Keller and Pardo, 2004; Eldrett et al., 2014; Elderbak and Leckie, 2016). Evidence for the BOZ has been reported from the upper Cenomanian *Sciponoceras* biozone within the US parts of the WIS (the location of the Lohali Point, Gunnison Gorge, Rebeca Bounds and Billings Landing sites), however evidence is absent, or rare, in the Canadian parts of the WIS, such as where the Pratts Landing site is located (e.g. Eicher and Worstell, 1970; Eicher and Diner, 1985; Leckie et al., 1991, 1998; Schröder-Adams et al., 1996; Elderbak et al., 2014; Elderbak and Leckie, 2016).

Oceanographic models for the US part of the WIS suggest the BOZ was caused by the interplay of different water masses, driven by sea-level variations. OAE2 occurred within the eustatic 3rd-order Greenhorn transgression (Fig. 2; Hancock and Kauffman, 1979; Kauffman and Caldwell, 1993; Gale et al., 2008). During the early stages of transgression the basin was relatively restricted and shallow, with low polar to tropical temperature gradients causing sluggish, stratified and low-oxygen conditions (Eicher and Diner, 1985; Kump and Slingerland, 1999; Allison and Wells, 2006). As the transgression progressed, a southern sill was breached and an influx of Tethyan waters to the east resulted in a strong Boreal-Tethyan oceanographic front in the seaway that may have extended from the central US to as far north as southern Canada (Fisher et al., 1994; Arthur and Sageman, 2005; Elderbak and Leckie, 2016; Lockshin et al., 2017; Bryant et al., 2021). The density differences between the southern saline, oxygen-poor Tethyan and northern, less-saline, oxygen-rich Boreal waters resulted in the creation of a third, denser water mass at the mixing front (a process called caballing), termed the Western Interior Intermediate Water (Hay et al., 1993). The denser water mass then sank, downwelling oxygenated surface waters, creating strong bottom-water currents, disrupting any benthic anoxia that may have been present, and resulted in the BOZ (Eicher and Worstell, 1970; Eicher and Diner, 1985; Elderbak and

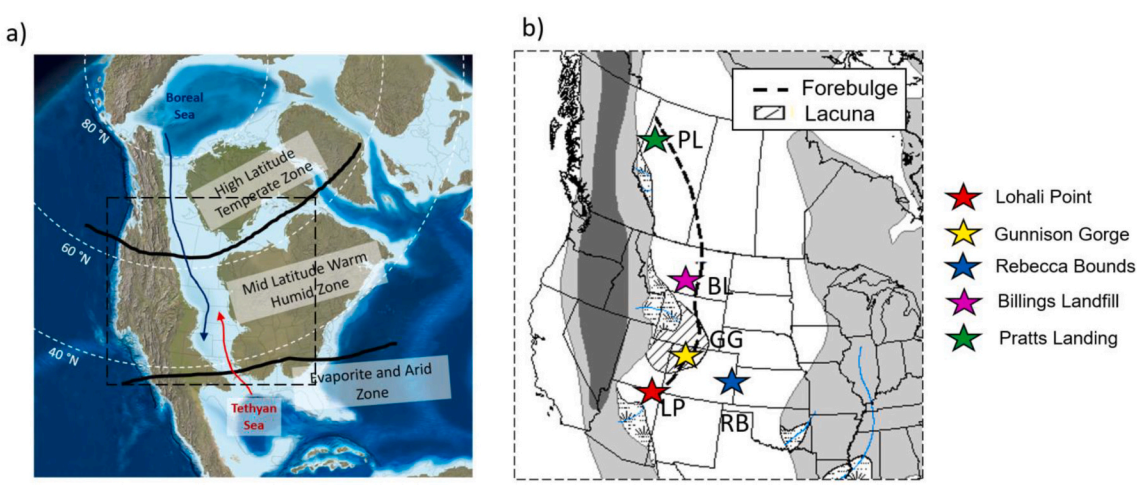

Fig. 1. Palaeogeography of, and study locations in, the Western Interior Seaway. a) Palaeogeographic map depicting climate zones across the Western Interior Seaway in the Cenomanian (~94 Ma to ~100 Ma), modified from Hay and Flögel (2012). Red line indicates the southern-sourced Tethyan water and the blue line represents the northern-sourced Boreal water. The dashed box represents the location for Fig. 1b. b) Location of the five study sites in the Cenomanian–Turonian WIS, with proposed location of lacuna (area of non-deposition) and forebulge. (For interpretation of the references to colour in this figure legend, the reader is referred to the web version of this article.)

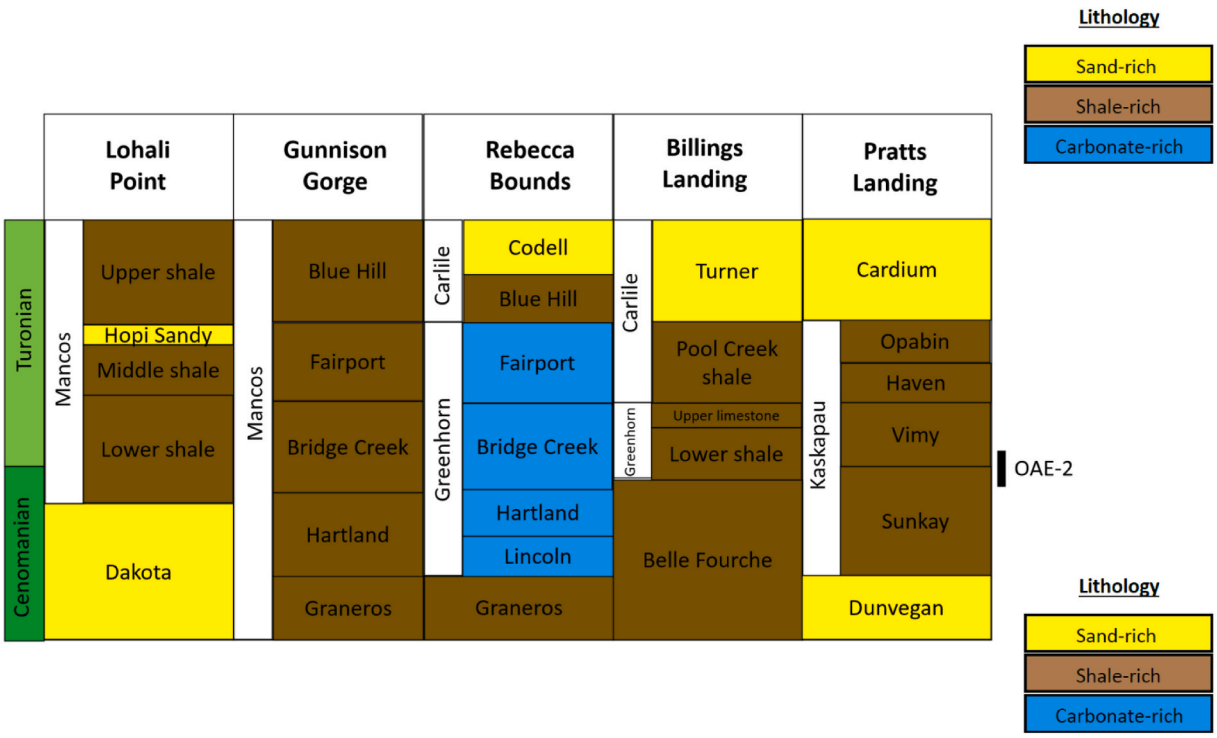

Fig. 2. Lithostratigraphic log of Lohali Point (Bralower and Bergen, 1998; Leckie et al., 1991; Kirkland, 1991), Gunnison Gorge (Noe, 2015), Rebecca Bounds core (Kennedy et al., 2005), Billings Landfill (Leckie and Leithold, unpublished) and Pratts Landing (Varban and Plint, 2008).

Leckie, 2016; Lowery et al., 2018; Bryant et al., 2021). Driven by the density differences of these water masses and freshwater influx from the hinterland, a counter-clockwise semi-estuarine circulation has been proposed to have occurred during the highest sea-levels (Slingerland et al., 1996; Floegel et al., 2005; Elderbak and Leckie, 2016; Lowery et al., 2018). Foraminiferal studies in Kansas (Elderbak et al., 2014; Lowery et al., 2018) support this model and suggest increased anoxia to the south east, and the influence of oxygen-poor Tethyan water.

Following the BOZ interval, dysoxic to anoxic conditions again prevailed in the US part of the WIS, as sea-level continued to rise and increased volumes of oxygen-poor Tethyan water were transported into the seaway (Lowery et al., 2018). The increased abundance of low-oxygen favouring *Planoheterohelix* foraminifera (termed the '*Heterohelix* shift' by Leckie et al., 1998) is noted at many sites, attributed to an expanded Oxygen Minimum Zone (OMZ) influenced by low-oxygen Tethyan waters (Leckie et al., 1991) and/or increased productivity (Boudinot et al., 2020).

The Canadian part of the WIS experienced different oceanographic conditions, and was likely cooler and less saline (Schröder-Adams et al., 1996). This, coupled with the stratified and anoxic conditions indicated by geochemical redox proxies, culminated in low abundances of agglutinated benthic foraminifera and an absence of bioturbation (Schröder-Adams et al., 1996; Simons et al., 2003). As sea-level rose through the late Cenomanian to early Turonian, planktic foraminifera and nannofossils appeared at some southern Canadian sites, signalling the influence of more normal saline marine Tethyan waters (McNeil and Caldwell, 1981; Caldwell et al., 1993; Schröder-Adams et al., 1996; Dionne et al., 2016). However, abundance and diversity was low, interpreted to be due to stable stratification (perhaps enhanced by a freshwater lid), anoxic conditions and inhospitable conditions for benthic or planktic fauna to thrive (Schröder-Adams et al., 2001; Schröder-Adams, 2014; Dionne et al., 2016). The oceanographic mixing front and caballing effect are not interpreted to have reached the Canadian part of the WIS (Dameron et al., n.d.).

1.2. Sample sites

To facilitate an integrated study, five sites spanning different water depths, palaeoenvironments and palaeolatitudes were selected (Table 1).

1.3. Organic geochemistry of the WIS

Lipid biomarkers provide insights into oxygenation, drivers of organic enrichment and perturbations of the carbon cycle (e.g., Eglinton and Eglinton, 2008; Peters et al., 2005). Previous studies of OAE2 within the WIS that include lipid biomarker analysis are primarily localised within the southwestern and central part of the basin (Curiale, 1994; Pancost et al., 1998; Simons and Kenig, 2001; Sun et al., 2016; French et al., 2019; Boudinot et al., 2020; Forkner et al., 2021), or within Alberta and Saskatchewan (Simons et al., 2003; Furmann et al., 2015). Many studies support the model of increased oxygenation during the onset of OAE2, or at the Cenomanian/Turonian boundary (CTB: Simons and Kenig, 2001; Sun et al., 2016; French et al., 2019; Forkner et al., 2021). Whilst foraminiferal studies indicate Tethyan-influenced anoxia to the southeast of the WIS, lipid biomarker proxies show regional variations with heightened anoxia and photic zone euxinia in some proximal locations on the western part of the basin (e.g. Pancost et al., 1998; Boudinot et al., 2020) and Canadian sites show high levels of anoxia independent of Tethyan water influence (Simons et al., 2003). Anomalously high concentrations of C_{28} steranes, interpreted to indicate an abundance of prasinophytes (simple unicellular green algae, often present in abundance under stressed environmental conditions, although other sources for C_{28} steranes such as chlorophyll *c*-containing algae are recognised: Volkman et al., 1994, 1998), suggest generally inhospitable environmental conditions linked to anoxia at sites across the WIS (Curiale, 1994; French et al., 2019; Boudinot et al., 2020; Robinson et al., in prep). There remain unresolved questions in these organic geochemical datasets, relating to the heterogeneity of anoxia across the basin and the significance of high C_{28} sterane concentrations,

Table 1
Key characteristics of the five sites studied here. Geographical latitude and longitude are given, with the number of significant figures representative of the known accuracy of the co-ordinates. For further details and references please see Supplemental Material A.

Site	Present-day Location	Palaeo latitude	Water depths	Depositional environment
Lohali Point (Outcrop)	36.183°N, 109.883°W (NE Arizona)	~43°N	< 100–200 m	Neritic environment, at the distal end of a broad, shallow, seaward-sloping shelf, and inwards of the forebulge trend
Gunnison Gorge (Outcrop)	38.7827°N, 107.86898°W (W Colorado)	~46°N	0–50 m	Proximal site that was located on a large palaeo-bathymetric high, created by the rising basin forebulge
Rebecca Bounds (Core)	38.489628°N, 101.974552°W (W Kansas)	~45°N	< 200–300 m	Distal axial basin
Billings Landfill (Outcrop)	45.72°N, 108.56°W (S Montana)	~55°N	< 100 m	Proximal location inwards of the basin forebulge
Pratts Landing (Outcrop)	56.020556°N, 118.813056°W (NW Alberta)	~64°N	< 70 m	Close to the forebulge, on the eastern flank of the foredeep, approximately 160 km from the WIS shoreline

that this study aims to address.

2. Methods

This study applies organic geochemical methods (i.e., lipid biomarker analysis) to investigate five sample sites across the KWIS. This is supplemented by bulk isotopic and elemental analysis, palynology, micropaleontology, and statistical analysis. Table 2 details the key lipid biomarker and supporting palynofacies proxies used, with additional detail about these proxies contained within Supplemental Material B. A detailed description of the methods is contained with Supplemental Material C.

3. Results and discussion

3.1. Thermal maturity of studied sections

Prolonged thermal stress, such as experienced during diagenesis, can rearrange the stereochemical configurations of steranes and terpanes until a critical point whereby the proportion of each isomer achieves a thermodynamically balanced distribution (Peters et al., 2005). Thus it is possible to ascertain thermal maturity through certain biomarker ratios (Peters et al., 2005; Table 3). Consistent with low thermal maturity, the 17β(H),21β-homohopane (C31ββ hopane) and 17β(H),21β hopane (C30ββ hopane) isomers are predominant (Ourisson et al., 1979; Peters and Moldowan, 1991; Seifert and Moldowan, 1981; Mackenzie et al., 1980), and the C31 αβ / (αβ + ββ) ratio, is relatively low <0,50. All locations studied here are thermally immature with respect to oil generation, and therefore geochemical proxies can be assumed to be representative of palaeoenvironmental conditions at the time of deposition.

3.2. Sample sites

3.2.1. Lohali Point

At Lohali Point, a positive carbon isotope excursion (CIE) of 3.3‰ (from −26.0‰ to −22.7‰) spans 15 m between 5 and 20 m height (Fig. 3B). Kirkland (1996) notes a disconformity at the CTB, however, the shape of the Lohali Point CIE is similar to that of other sites and key features (such as the peak-trough-peak-plateau shape: Pratt and Threlkeld, 1984) are also present. We thus propose that the record is largely complete.

Increased foraminiferal abundance through the section suggests increasing sea-level through the section and maximum transgression in the lower Turonian *Mammites nodosoides* to perhaps the basal *Collignoniceras woollgari* biozone (Leckie et al., 1991, 1998). Proxies for terrestrial organic matter (oleanane index and TAR - Fig. 3C) also increase up-section which is not the usual trend seen with transgression when shorelines and terrestrial matter delivery systems are shifted further away. Clay mineral, sedimentological and foraminiferal data suggest increased weathering during this time (Leckie et al., 1991), driven by an enhanced global hydrological cycle (van Helmond et al., 2014), and perhaps locally driven by the increase of latent heat into the seaway from the northwards incursion of warm waters (Leckie et al., 1991), explaining the increase in delivery of terrestrial OM up-section. There are, however, relatively low values for all terrestrial proxies, which agrees with the assessment of Leckie et al. (1991) who found minimal presence of plant debris in the Lower Mancos foraminiferal residues despite high sedimentation rates. This suggests that the hinterland by Lohali Point was potentially arid and thus lacking significant vegetation cover, which may have increased the susceptibility of the hinterland to weathering during times of increased rainfall.

Values of Pr/Ph vary little (average 0.85 - Fig. 3E) through the section, indicating generally anoxic conditions. The elevated values of the C_{34}/C_{35} HH proxy indicate more oxygenated conditions in the first ~11 m, and coincide with an increase in foraminiferal species richness and the BOZ identified at 5–11 m (*Sciponoceras biozone)* (Leckie et al., 1998). Overall however this site shows low benthic and planktic foraminiferal diversity, particularly compared to the central part of the seaway at this time (Leckie et al., 1998; West et al., 1998).

Above 11 m, and mid-way through the CIE, a trend to anoxic depositional conditions corresponds to an increase in isorenieratane derivatives, gammacerane and C_{28} sterane abundance (Fig. 3G-I). This coincides with an increased abundance of *Planoheterohelix* foraminifera ('*Heterohelix* shift') indicating the presence of oxygen-poor waters (Leckie et al., 1991).

3.2.2. Gunnison Gorge

The Gunnison Gorge section has been dated using nannofossil biostratigraphy, highlighting a disconformity within a prominent ~8 cm limestone bed with an erosive base and mud rip-up clasts (see Supplemental Material A: Sample Sites). The switch from biota that have their last occurrence early in the CIE (e.g. *L. acutus* and *C. kennedyi*) to those that have their first occurrence late in the CIE (*E. moratus/eptapetalus*) suggest that at least the mid-part of the CIE (e.g., between 20.9 and 21.5 m height; Fig. 4) is missing in this section. Here, a dramatic shift is seen in nearly all the proxy data, and the $\delta^{13}C_{org}$ CIE is not recorded (Fig. 4B).

Despite a disconformity at the CIE, this site is still useful for determining the changing conditions before and after OAE2. Before the hiatus (i.e., before OAE2), sediments are generally lower in $CaCO_3$ and TOC (Fig. 4A, average 16% and 1.5% respectively), with values for both parameters decreasing to just before the disconformity. Low gammacerane values (Fig. 4G) indicate a possible lack of water column stratification, and increased Pr/Ph and C_{34}/C_{35} HH (Fig. 4E) suggest anoxia was not prevalent at this site and the site was in fact becoming more oxygenated just before the disconformity. This, coupled with a slight decrease in C_{28} sterane abundance (Fig. 4H), suggest well ventilated and habitable waters just prior to the disconformity.

After the disconformity (i.e., after OAE2), a decrease in Pr/Ph and C_{34}/C_{35} HH values suggest less oxygenated, but not anoxic, conditions.

Table 2
Geochemical and palynological proxies used in this study.

Indicator	Tech-nique	Proxy	Description	Ref.
Terrestrial input	Lipid biomarkers	**TAR** (Terrigenous Aquatic Ratio) *($nC_{27} + nC_{29} + nC_{31}$)/ ($nC_{17} + nC_{19} + nC_{21}$)*	Higher TAR indicates more input from the terrigenous-derived C_{27}, C_{29} and C_{31} n-alkanes.	(Peters et al., 2005)
		Oleanane Index *(oleanane / [oleanane + C_{30} αβ hopane])*	Derived from angiosperms (flowering plants).	(Riva et al., 1988; Moldowan et al., 1994)
	Palynofacies	**C/M** *(no. terrestrial phytoclasts + pollen + spores) / (no. of dinocysts, prasinophytes, acritarchs) *with the exception of Pratts Landing (see 1.4.3 Palynology)*	% organic matter derived from terrestrial plants, compared to all terrestrial and marine organic matter	(Tyson, 1995)
Redox	Lipid biomarkers	**Pr/Ph** *(pristane/ phytane)*	Phytane is preferentially preserved in anoxic settings. Broadly: <~1 anoxic, >3 oxic	(Didyk et al., 1978; Ten Haven et al., 1987)
		C_{34}/C_{35} HH *(C_{34}αβ R/C_{35}αβ R homohopane)*	C_{35} hopane is preferentially preserved in anoxic settings. <~1 anoxic	(Peters et al., 2005)
		Isorenieratane *(P = present; T = trace; A = Absent)*	Produced by anaerobic brown-pigmented green sulfur bacteria in the photic zone. Presence indicates photic zone euxinia.	(Grice et al., 1996)
Strat-ification	Lipid biomarkers	**Gammacerane Index** *(gammacerane / [gammacerane + C_{30} αβ hopane])*	Most often attributed to ciliates at a chemocline in the water column, although the precursor for gammacerane (tetrahymanol) has other sources such as photosynthetic bacteria and freshwater ciliates.	(Sinninghe Damsté et al., 1995; Peters et al., 2005)
Ecological change	Lipid biomarkers	**Sterane / Hopane** *(ratio of regular ααα steranes over regular hopanes)*	Ratio of molecules of eukaryotic (primarily algal / or plant) / bacterial origin	(Peters et al., 2005)
		Sterane abundance *relative abundance of ααα R isomers*	Derived from eukaryote sterols, with C_{27}, C_{28}, C_{29} representing differing precursor organisms.	(Volkman, 2003)
	Paly-nofacies	**Prasinophyte** *% no. prasinophytes / total no. of particles counted in sample*	Simple unicellular green algae, often present in abundance under harsh environmental conditions	(Tappan, 1980; Tyson, 1995)

A stark shift is seen in C_{28} sterane abundance, however, with C_{28} representing twice that of the C_{27} or C_{29} component. TOC also increases to highs of 5.2%, but values show some variability based upon the fluctuating $CaCO_3$ component. A general increase in terrestrial proxies is seen during this interval, including variability within the TAR and the presence of wood preserved as jet. Alongside variable $CaCO_3$, this suggests a dynamic and fluctuating palaeoenvironment driven by relative sea-level and/or pulses of fluvial input.

3.2.3. Rebecca Bounds core

The CIE is clearly seen in the Rebecca Bounds core (Fig. 5B), with $\delta^{13}C_{org}$ values increasing by 4.3‰ from −27.3‰ to −23.0‰ (Fig. 5A). The excursion follows the same trend as other $\delta^{13}C_{org}$ isotope curves published for this location (Scott et al., 1998; Sageman et al., 2006; Joo and Sageman, 2014), including the presence of subpeaks that are commonly seen in CTB $\delta^{13}C_{org}$ records across the WIS (Pratt and Threlkeld, 1984; Pratt, 1985).

$CaCO_3$ values are relatively high, with an average of 55.5%. TOC values fluctuate between 1.1% and 6.9%, with pronounced variation during the CIE (Fig. 5A). Terrestrial proxies TAR, Oleanane index and C/M (Fig. 5C) suggest fluctuating terrestrial organic matter input with a decrease in the later part of the CIE up to the middle part of the Bridge Creek Limestone Member.

Pr/Ph values suggest that this site was not particularly anoxic, and although there are particularly low C_{34}/C_{35} HH values (Fig. 5E) these are likely due to high amounts of C_{35} homohopanes associated with carbonate lithologies (Peters et al., 2005). All redox proxies (Pr/Ph, C_{34}/C_{35} HH, isorenieratane – Fig. 5E-F) indicate increased oxygenation at the start of the CIE, continuing until the middle part of the Bridge Creek Limestone, where proxies indicate a slight decrease in oxygenation upcore. Gammacerane values are low, but suggest possible stratification before the CIE, with stratification less likely from the CIE up to the top of the section (Fig. 5G). A switch from C_{28} being the major to the minor component of the steranes occurs at the base of the CIE, however, C_{28} then becomes dominant again at the end of the CIE (Fig. 5H).

3.2.4. Billings Landfill

The CIE at Billings Landfill is identified as a ~ 3‰ positive excursion in $\delta^{13}C_{org}$ values from the *Sciponoceras* ammonite biozone and extending to the *Watinoceras* ammonite biozone (Fig. 6B). Erosive surfaces are seen at outcrop immediately prior to the CIE and a comparison of the shape of the excursion with other isotopic expressions of OAE2 from the WIS show a condensed, or truncated, onset of the CIE (Dameron et al., n.d.).

$CaCO_3$ is relatively low from the base of the section, rising from ~5 to ~15% $CaCO_3$ in the lower 35 m (Fig. 6A). After 35 m $CaCO_3$ increases to an average of 26%, concurrent with a dominance in *Neobulimina* calcareous benthic foraminifera (Dameron et al., n.d.). TOC is also relatively low, dropping from ~1.5% to lows of 0.2% in the lower part of the CIE before rising again to values ~1.5% in the upper part of the CIE and above (Fig. 6A). The initial decrease in TOC values coincides with the BOZ identified by foraminiferal workers (Dameron et al., n.d.). Oleanane and C/M values suggest a significant input of terrestrial organic matter at this time (Fig. 6C-D), which may indicate increased run-off and clastic dilution of organic matter, contributing to the low TOC values.

Table 3
Biomarker maturity parameters for five study sites.

Parameter	Approx. values for maturity	Lohali Point (n = 36)	Gunnison Gorge (n = 31)	Rebecca Bounds (n = 44)	Billings Landfill (n = 50)	Pratts Landing (n = 40)
Ts / (Ts + Tm)	1 = late oil	0.16 ± 0.09	0.28 ± 0.09	0.31 ± 0.09	0.16 ± 0.04	0.32 ± 0.06
C_{29} Sterane 20S / (20S + 20R)	0.55 = peak oil	0.06 ± 0.02	0.24 ± 0.03	0.04 ± 0.02	0.12 ± 0.03	0.11 ± 0.06
C_{30} Hopane / (Hopane + Moretane)	0.95 = early oil	0.65 ± 0.06	0.77 ± 0.04	0.73 ± 0.05	0.72 ± 0.02	0.69 ± 0.1
C_{32} Hopane 22S / (22S + 22R)	< 0.6 = immature	0.17 ± 0.05	0.52 ± 0.02	0.24 ± 0.1	0.39 ± 0.02	0.36 ± 0.09

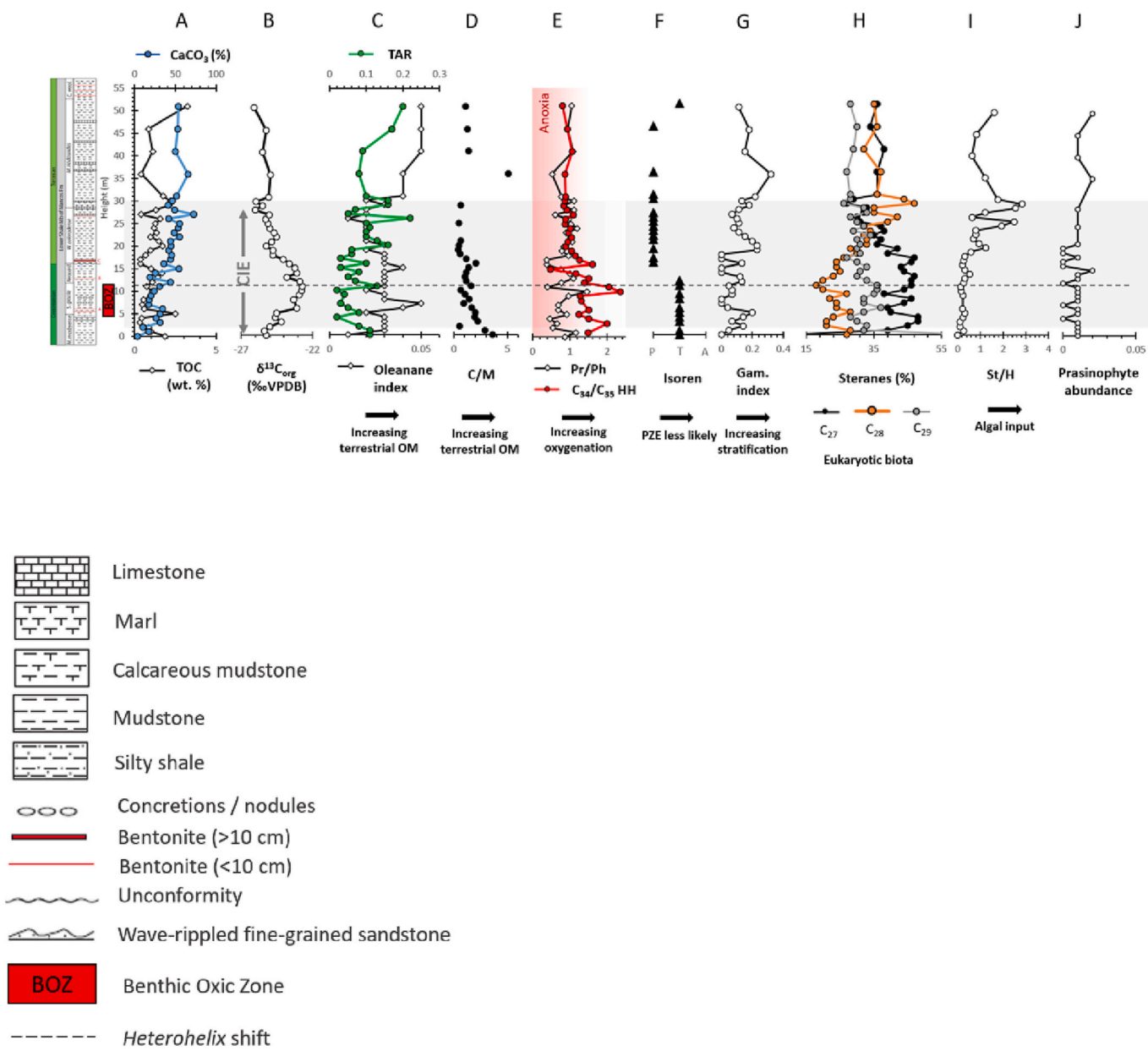

Fig. 3. Geochemical results for the Lohali Point site: TOC (wt%), $CaCO_3$ (%), $\delta^{13}C_{org}$ (‰VPDB), TAR (terrigenous aquatic ratio: ($nC_{27} + nC_{29} + nC_{31}$)/ ($nC_{17} + nC_{19} + nC_{21}$)), Oleanane index (oleanane / (oleanane + C_{30} αβ hopane)), C/M (continental/marine: (no. terrestrial phytoclasts + pollen + spores) / (no. of dinocysts, prasinophytes, acritarchs)), Pr/Ph (pristane/phytane), C_{34}/C_{35} HH ($C_{34}\alpha\beta$ R/$C_{35}\alpha\beta$ R homohopane), Isoren (presence of isorenieratane: Present, Trace, Absent), Gam. index (gammacerane / (gammacerane + C_{30} $\alpha\beta$ hopane)), Steranes (relative abundance of steranes where C_x = 100 * (C_x aaaR /(C_{27} aaaR – C_{29} aaaR))), St/H (ratio of selected regular steranes over hopanes) and prasinophyte abundance. For further details on the proxies used, refer to Table 1 and Supplemental Material B. Data points are not joined for C/M and Isoren as not every sample was analysed for these proxies. Ammonite zonation, Benthonic Zone (red box) and Heterohelix shift (dashed line) are taken from Leckie et al. (1991, 1998). (For interpretation of the references to colour in this figure legend, the reader is referred to the web version of this article.)

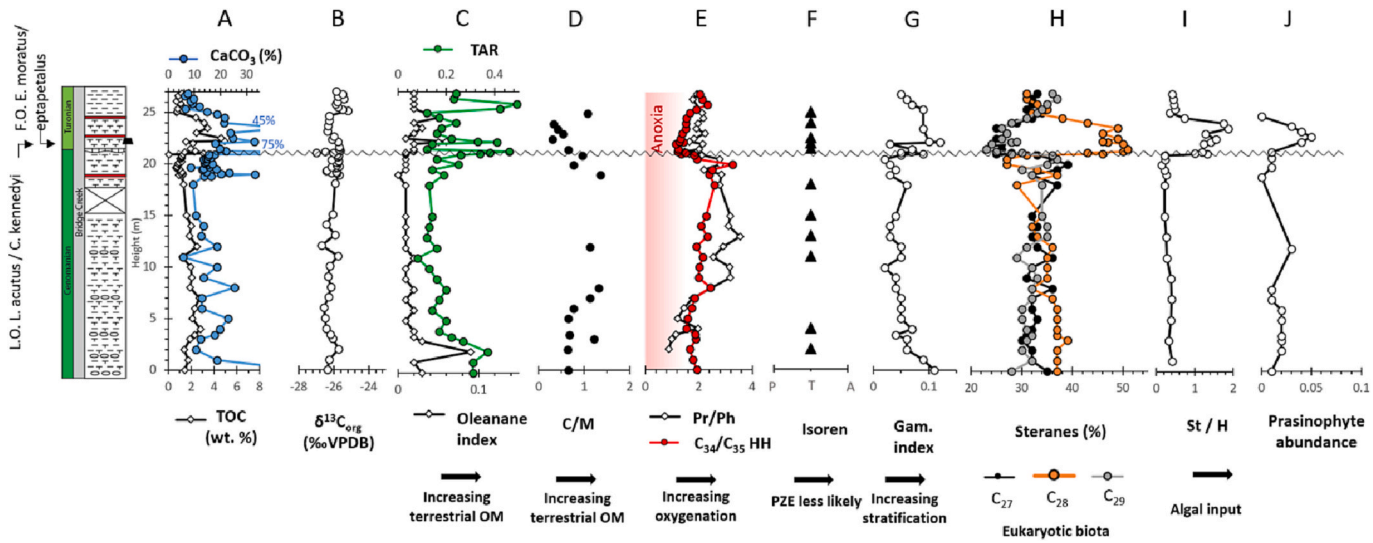

Fig. 4. Geochemical results for the Gunnison Gorge site. See Fig. 3 for proxy and sedimentary log key. For further details on the proxies used, refer to Table 1 and Supplemental Material B. Last and first occurrences of selected nannofossils displayed.

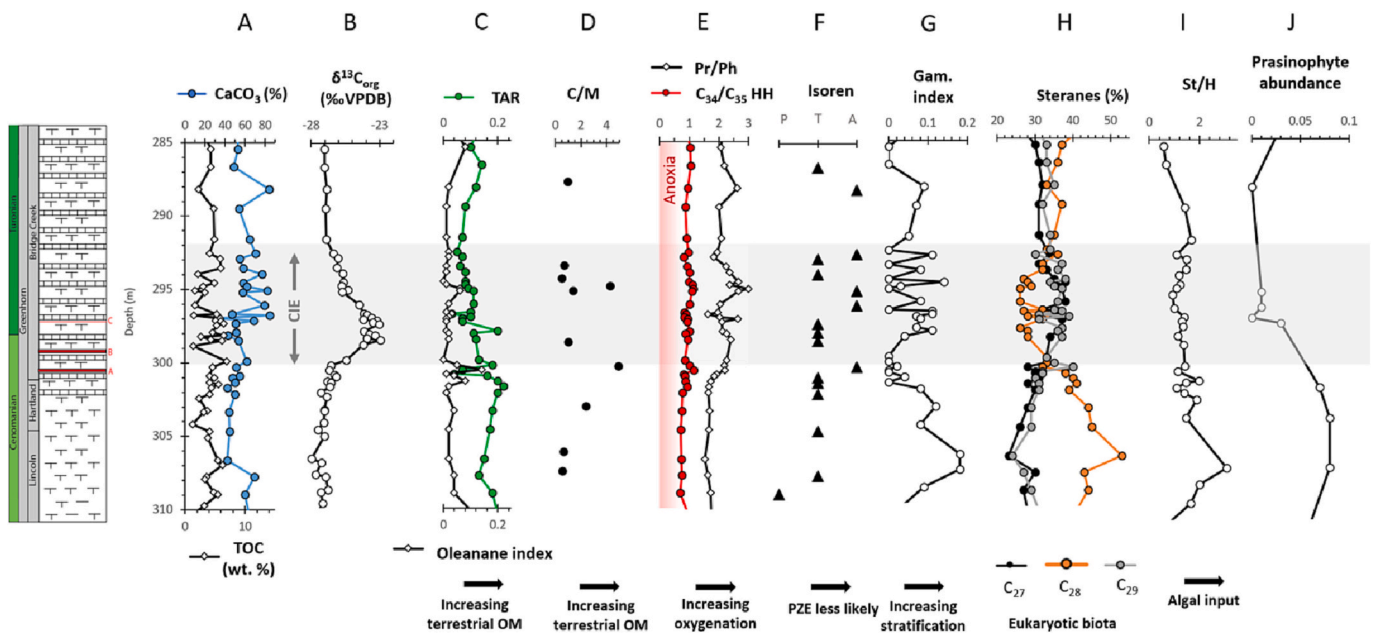

Fig. 5. Geochemical results for the Rebecca Bounds core. See Fig. 3 for proxy and sedimentary log key. Major bentonites A, B and C are marked on the sedimentary log in the lower Bridge Creek Member. For further details on the proxies used, refer to Table 1 and Supplemental Material B.

Pr/Ph and C_{34}/C_{35} HH suggest an overall oxic to dysoxic site (Fig. 6E). Both ratios show a decrease in oxygenation to possible anoxic to dysoxic conditions between 21 and 30 m height during the lowermost part of the CIE, corresponding with an increase in terrestrial organic matter and gammacerane. A discrete interval of greater foraminiferal abundance and diversity represents a BOZ in the lower part of the section (19.5–20.5 m: Dameron et al., n.d.), which, although brief, does coincide with a stark decrease in C_{28} sterane abundance for ~4 m, and absence of photic zone euxinia indicator isorenieratane (Figs. 6F and H).

3.2.5. Pratts Landing

At Pratts Landing, a disconformity during the lowermost Turonian has been inferred from wireline correlation (van Helmond et al., 2016). This disconformity is represented in the CIE at the CTB by a sharp drop in δ $^{13}C_{org}$ values in what would have been the plateau of the CIE (Fig. 7B). The start of the CIE is located within the sandstones in the upper part of the Sunkay Member and has an overall positive shift of 2 ‰.

$CaCO_3$ values for samples throughout this site are below detection limit. TOC values are low through the silty and sandy Sunkay Member (0–14 m, average 0.8%), rising to 4.8% in the claystone of the lower part of the Vimy Member (14–15 m: Fig. 7A). A sharp and significant increase is seen in TOC values, from 2.6 to 14%, above the hiatus in the Vimy Member at approximately 15 m.

Terrestrial proxies (oleanane, TAR and C/M – Fig. 7C-D) show discrete increases in terrestrial organic matter corresponding to particularly low TOC values between 5 and 5.5 m and 19–22 m height, within the wave-rippled fine-grained sandstones of the Sunkay Member and the Vimy member respectively. The oleanane index is low throughout the section, despite relatively high TAR values and coarse-grained facies indicating close proximity to shore. Although angiosperms had radiated to Arctic latitudes by the mid-Cenomanian (Upchurch and Wolfe, 1993),

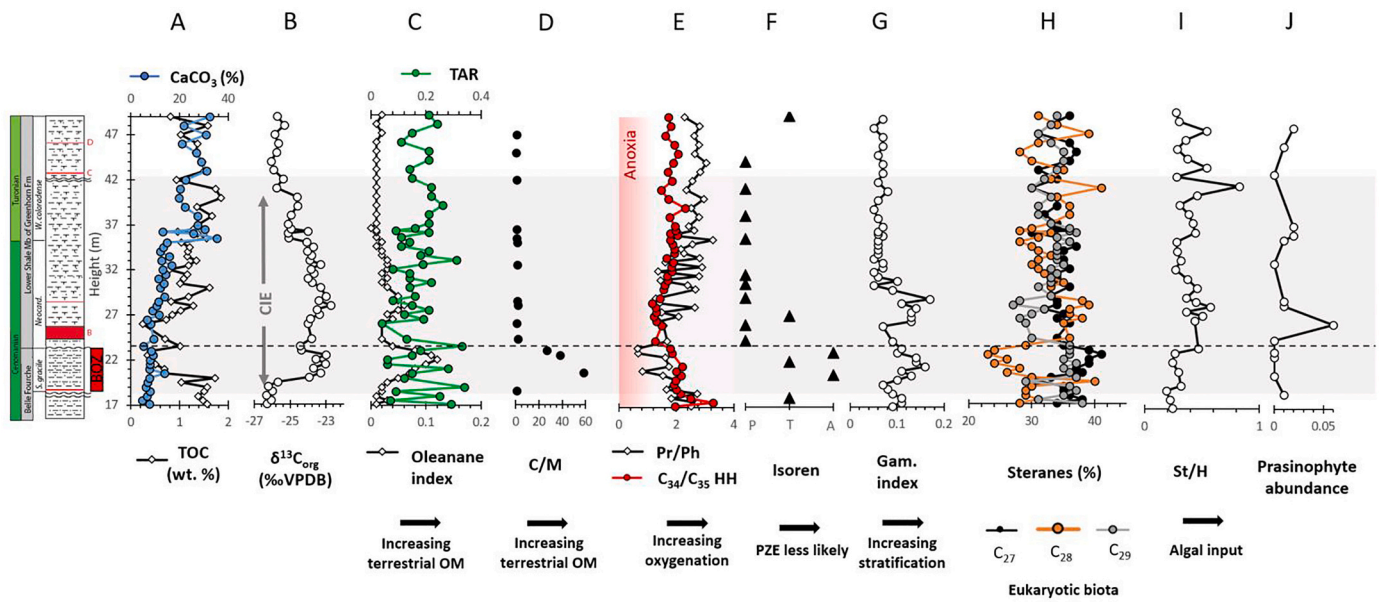

Fig. 6. Geochemical results for the Billings Landfill site. See Fig. 3 for proxy and sedimentary log key. For further details on the proxies used, refer to Table 1 and Supplemental Material *B. major* bentonites A, B, C and D are marked on the sedimentary log in the lower shale member of the Greenhorn Formation. Ammonite zonation, Benthonic Zone (red box) and Heterohelix shift (dashed line) are taken from Dameron et al., n.d.. (For interpretation of the references to colour in this figure legend, the reader is referred to the web version of this article.)

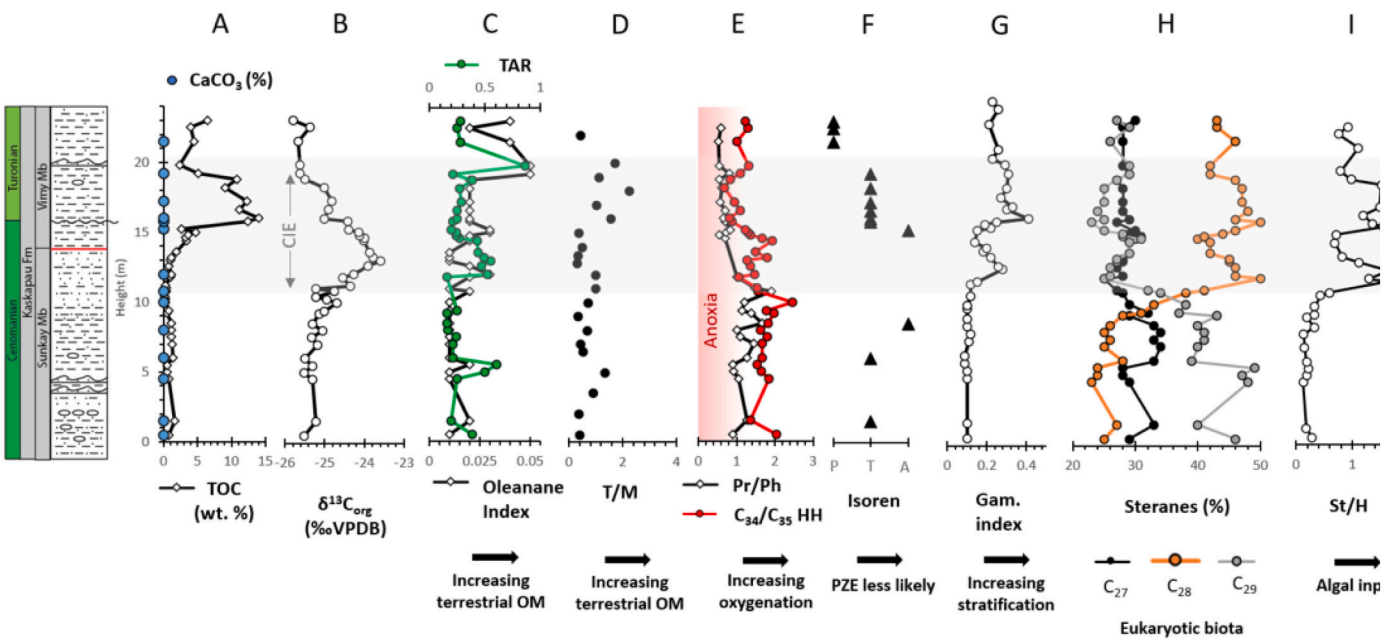

Fig. 7. Geochemical results for the Pratts Landing site. See Fig. 3 for proxy and sedimentary log key. For further details on the proxies used, refer to Table 1 and Supplemental Material B. Prasinophyte data were not collected for this section.

these oleanane values suggest they were unlikely to be in abundance in the hinterland close to Pratts Landing.

Some Pr/Ph values were not recorded in this section due to loss of shorter chain *n*-alkanes, identified by the chromatogram profile which would have resulted in depressed and non-representative Pr/Ph values. This occurs most often in the upper part of the Sunkay Member and may be related to the low organic content in these sandstones. The Pr/Ph trend for non-degraded samples, however, does match with that of the C_{34}/C_{35} HH, taken from larger-chain terpanes, indicating that values here are likely representative of redox conditions (Fig. 7E).

Low gammacerane and C_{28} steranes values below the CIE in the Sunkay Member, coupled with elevated values for redox proxies (Pr/Ph and C_{34}/C_{35} HH) and elevated C_{29} steranes, indicate an oxygenated, mixed water column with the largest eukaryotic component deriving from land plants (Fig. E, G, H). At the onset of the CIE however oxygenation decreases, stratification increases and C_{28} sterane values dramatically rise from 26 to 50% abundance through the lower part of the Vimy Member to the disconformity. Above the disconformity redox proxies are at their lowest (Pr/Ph averaging 0.63; C_{34}/C_{35} HH averaging 1). Above ~19 m height, a slight increase in C_{34}/C_{35} HH coincides with a lack of isorenieratane derivatives and decrease in TOC from 10.8 to 2.4%, alongside an increase in terrestrial organic matter and presence of

wave-rippled, fine-grained sandstones. Isorenieratane derivatives are only present in trace amounts, or are occasionally absent, indicating prolonged PZE was unlikely at this location (Fig. 7F).

3.3. Correlation, sedimentation rates and sea level

The five sites here can be correlated from the positive CIEs, volcanic ash layers (i.e. bentonites), published ammonite biozones, nannofossils and/or prominent carbonate beds (Elder, 1987; Bralower and Bergen, 1998; Elderbak and Leckie, 2016). TOC and $CaCO_3$ increase up section to maximum values above the CIE at all sites. This is interpreted to reflect a decrease in clastic input and increasing sea-level, and thus allowing a tentative positioning of the zone of maximum flooding (White and Arthur, 2006; Fig. 8).

Indications of missing time such as erosive surfaces and truncated carbon isotope curves are apparent for all proximal sites (i.e., Lohali Point, Gunnison Gorge, Billings Landfill, Pratts Landing; Fig. 8). Disconformities are found in the upper Cenomanian and CTB interval across the WIS, attributed to winnowing (caused by either sea-level fall or rise) and/or condensation due to sediment starvation during subsequent transgression (Sageman, 1996; Schröder-Adams et al., 1996, 2012; Varban and Plint, 2008; Eldrett et al., 2017). Oceanographic modeling suggests a strong, southward-flowing coastal jet impinged on the seafloor in the location of the NW Colorado High (Slingerland et al., 1996) which may explain the significant disconformity at the Gunnison Gorge location, leading to the loss of sediments deposited during OAE2. No evidence of missing strata/time is evident in the Greenhorn Formation in the more distal Rebecca Bounds core (Scott et al., 1998).

3.4. Terrigenous input

Terrestrial proxies in this study do not tend to correlate well with each other, a trend seen in other biomarker studies (Boudinot et al., 2020), and is likely due to differences in the source and transport mechanisms for terrigenous organic matter. Across its broad latitudinal extent, the WIS would have had multiple fluvial systems discharging into the basin, predominantly from the western coast where fluvio-deltaic systems transported clay-rich sediment and terrestrial organic matter from the rising Sevier mountains (e.g. Bhattacharya and Tye, 2004; Hay and Plint, 2020; Li et al., 2015; Plint, 2000), but also from the east (Elderbak et al., 2014).

Dominance of terrestrial over marine organic matter in a basin can be influenced by: (a) distance from the shoreline (moderated by relative sea-level); (b) transport pathways (e.g., hydrological cycle and wind); and (c) plant biomass on the hinterland. Low terrestrial proxy values generally correlate with high sea-level for the Gunnison Gorge, Rebecca Bounds and Pratts Landing sites, indicating relative sea-level (and therefore distance from shoreline) was driving terrestrial organic matter

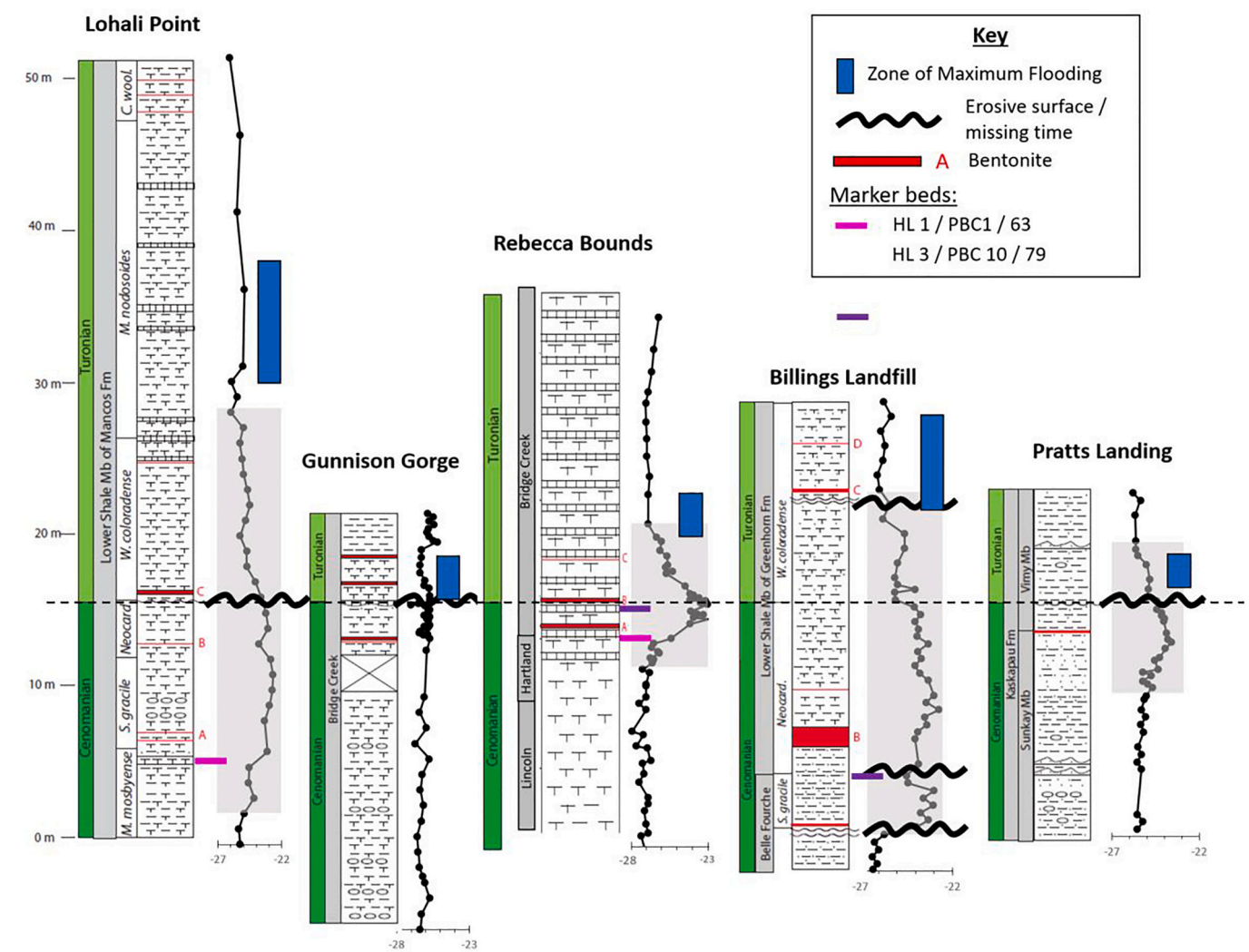

Fig. 8. Sedimentary logs and $\delta^{13}C_{org}$ isotope curve for the five study sites. Sedimentary log key is found in Fig. 3. Grey box indicates the CIE of OAE2. Marker beds use the nomenclature of Hattin (1985), Elder and Kirkland (1985) and Cobban and Scott (1972).

content. The opposite is apparent for Lohali Point, where increased hydrological cycling during rising sea-levels (Leckie et al., 1998; van Helmond et al., 2014) drove an increased contribution of terrestrial organic matter and overprinted any signal from sea-level variations.

3.5. C_{28} sterane abundance, prasinophytes and algal productivity

C_{27} and C_{29} steranes correlate with each other at each section and, with the exception of Lohali Point (Fig. 3H) and the pre-CIE section of Pratts Landing (Fig. 7H), show similar values. C_{28} sterane, however, covaries with both C_{27} and C_{29} suggesting that variations in C_{28} sterane drive the sterane signal (Figs. 3 – 7), similar to findings at other WIS sites (Supplemental Material F).

PCA was undertaken to elucidate primary controls on the drivers of proxy variation and organic matter composition and highlight relationships between the sterane and prasinophyte proxies (Fig. 9). In all

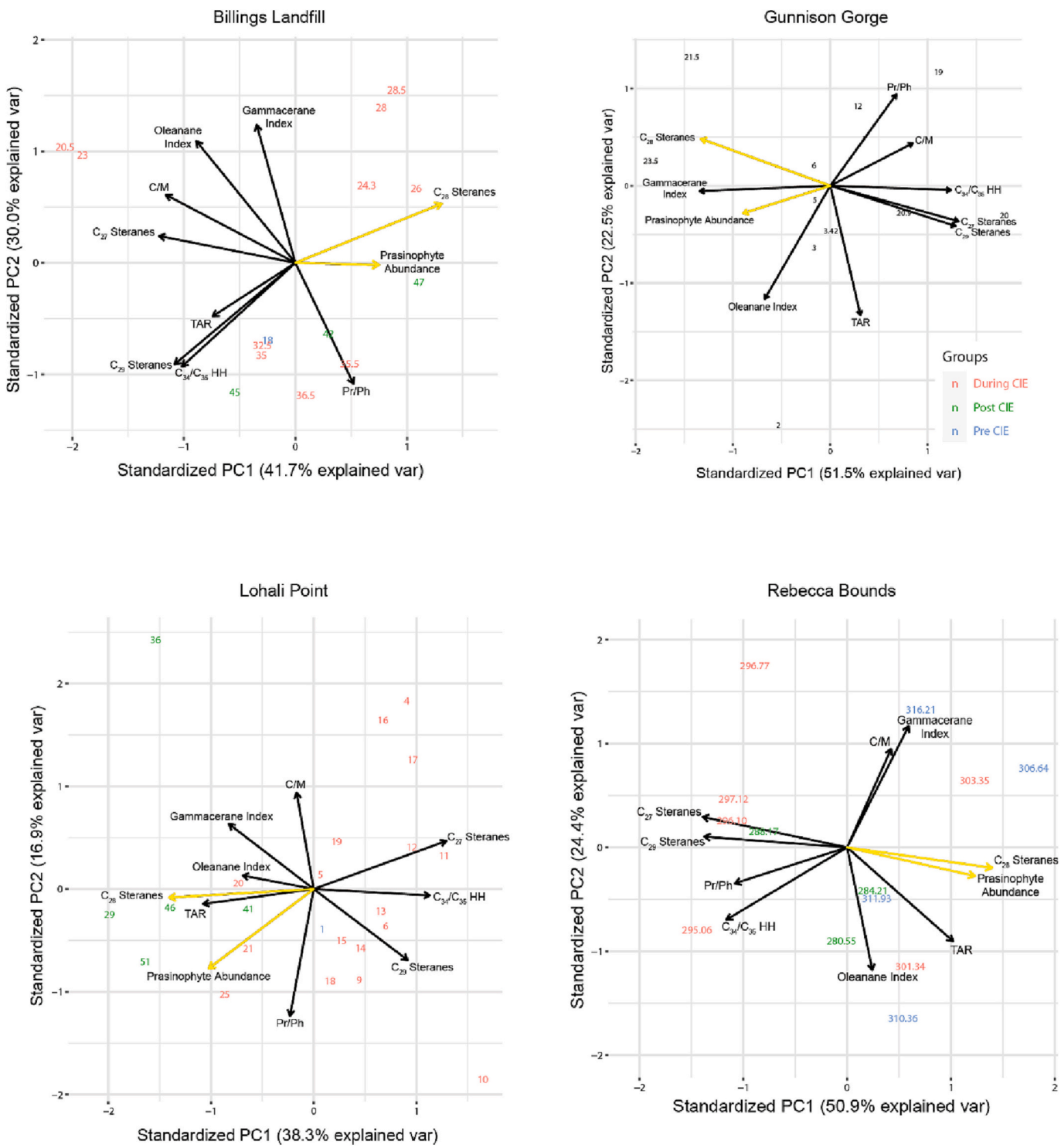

Fig. 9. Principal Components (PC) 1 and 2 for Billings Landfill, Gunnison Gorge, Lohali Point and Rebecca Bounds. Numbers represent specific depths/heights. Prasinophyte abundance and C_{28} sterane axes highlighted in yellow. Note that in each plot these axes plot close to each other, and typically contribute the most to PC1 (highest explained variance). (For interpretation of the references to colour in this figure legend, the reader is referred to the web version of this article.)

PCA plots the arrow vector for C_{28} sterane is approximately 180° to that of C_{27} and C_{29} sterane, further supporting the covariation between C_{28} sterane and C_{27} and C_{29} steranes by demonstrating that C_{28} sterane controls the variability in the data in opposing ways to C_{27} and C_{29} steranes.

Steroids are important components within all eukaryotic cell membranes, and their wide distribution in biological systems limits the capacity to use their diagenetic products, the sterenes, steranes and diasteranes, as biomarkers for specific organisms (Volkman, 1986). Definite phylogenic relationships can be established, however, with C_{27} steranes (cholestane) generally indicative of red-algae, C_{28} steranes (ergostane) of marine prasinophyte- and chlorophyll-*c* phytoplankton and C_{29} steranes (stigmastane) from freshwater or other marine green algae, and land plant material (Huang and Meinschein, 1979; Tissot and Welte, 1984; Volkman, 1986; Schwark and Empt, 2006; Knoll et al., 2007; Kodner et al., 2008). The relative compositions of these molecules have varied over deep time, recording major shifts in eukaryote ecology and evolution (Brocks et al., 2017).

C_{28} steranes may derive from numerous chlorophyll $a + c$ phytoplankton, such as Bacillariophyceae, Dinoflagellata, and Haptophyta (Falkowski et al., 2004; Volkman et al., 1998). Abundance of C_{28} steranes has been particularly linked to prasinophyte abundance however, and are the dominant sterane within living prasinophyte species that have been studied (Volkman et al., 1994; Schwark and Empt, 2006). Prasinophytes are unicellular green algae (Fig. 10) that have been considered 'disaster species' by Tappan (1980) due to their abundance in sediments deposited in low-oxygen conditions associated with environmental perturbations and biotic turnovers (e.g. van de Schootbrugge et al., 2005; Baranyi et al., 2016). Indeed, within this study high C_{28} sterane values correspond with less oxygenated conditions (Fig. 11), although the correlation is not of high statistical significance for most sites.

As displayed by the vector arrows protracting in near identical directions in the PCA results, C_{28} sterane and prasinophyte abundance proxies control variability in the data in very similar ways suggesting a relationship between the two proxies. In addition, in each plot the C_{28} sterane and prasinophyte abundance arrow vectors contribute to the Principal Component (PC)-1. This supports the positive relationship between the abundance of C_{28} steranes and prasinophytes at the Lohali Point, Gunnison Gorge, Billings Landfill and Rebecca Bounds sites (Figs. 3 – 6). Increased prasinophyte abundances identified from palynofacies analysis correlate with high C_{28} sterane values, although high C_{28} steranes can occur in samples with low prasinophytes (such as the lower part of the Gunnison Gorge section). This may indicate additional sources of C_{28} steranes from Chlorophyll-*c* producing organisms, such as red/brown algae and dinoflagellates (Dougherty et al., 1970), or the presence of nano- or pico- sized prasinophytes (<2 μm) too small to be retained by the 15 μm sieve used in palynological processing. The overall low abundance of prasinophytes identified within these samples must be acknowledged and may be due to said loss of nano- or pico-sized prasinophytes.

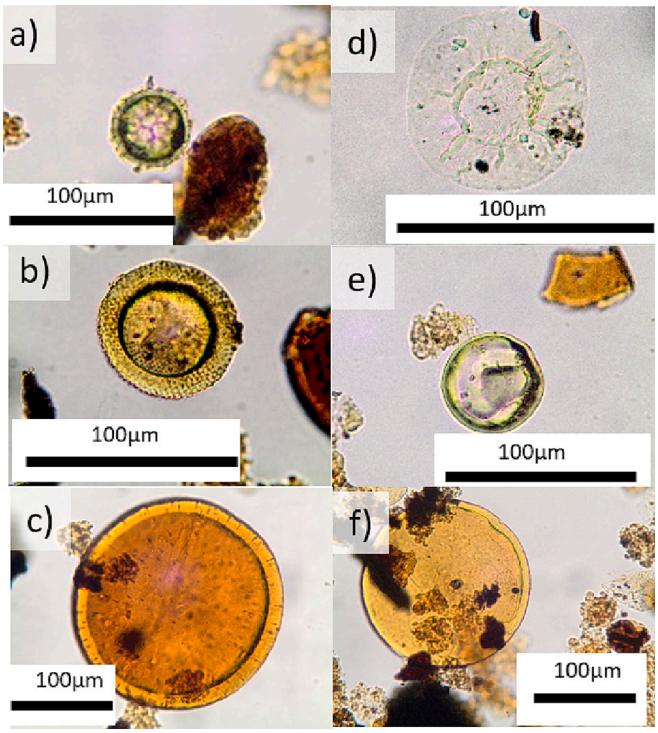

Fig. 10. Prasinophytes identified within this study; a) Herkomorph (?Cymatiosphaera); b) Tasmanitid (Lophosphaeridium); c) Tasmanitid (Crassospaera); d) Pteromorph; e-f) Leiosphere.

Comparing trends in our sterane data with the foraminiferal work conducted on Lohali Point (Leckie et al., 1998; West et al., 1998), shows that sterane trends reflect faunal variations. At Lohali Point, maxima in % planktic foraminifera at 3, 7 and 11 m correspond to maxima in C_{27} steranes and a minima in C_{28} sterane values. Furthermore, the *Heterohelix* shift at 11 m (base *Neocard.* biozone), indicative of an increase in low oxygen dwelling *Planoheterohelix globulosa*, marks a possible decrease in redox proxies, and coincides with the start of a steady increase in C_{28} sterane values.

C_{28} sterane trends show a strong coupling to the ratio of eukaryotic steranes to bacterial hopanes (St/H: Figs. 3 – 7) – indicating heightened algal presence due to prasinophyte abundance. Increased algal abundance is typically caused by high nutrient input and Forkner et al. (2021) and Zeng et al. (2018) postulate that episodic volcanism and associated nutrient influx drove variations in primary productivity during OAE2, as evidenced by an increase in C_{28} sterane above some bentonites. An anomalously high C_{28} value of 40% at above a bentonite at 19.4 m at Billings and elevated values up to 39% after Bentonite B (Fig. 6H) is demonstrated, with the latter coinciding with a significant increase in prasinophytes identified through palynology (Fig. 6J). There are also slight fluctuations in the steranes at Rebecca Bounds where C_{28} becomes the dominant sterane in an otherwise low C_{28} sterane trend (between depths of 297.32 m and 296.68 m) immediately after Bentonite B (Fig. 5H). These occurrences do not coincide with elevated St/H values, however, suggesting that whilst the overall eukaryotic community may become more dominated by prasinophytes, volcanic activity does not appear to drive increased algal productivity. In this study redox proxies do not vary significantly above bentonites, and so biogeochemical effects other than productivity-driven expansion of the OMZ (Zeng et al., 2018) must also be considered to account for the increase in prasinophytes, such as volcanic-driven water-column toxicity (e.g. Cronin et al., 2003), a change in pH (Wang et al., 2021), decreased irradiance and/or other climate/environment shifts.

The strong correlation seen between C_{28} sterane and gammacerane in this study indicates that stratification may be a major driver of algal activity in the WIS. Gammacerane is derived from tertrahymanol, which is primarily biosynthesised by bacterivorous ciliates in the absence of steroid-rich algae at the interface between oxic and anoxic zones in stratified water columns (Li, 1989; Ten Haven et al., 1989; Sinninghe Damsté et al., 1995). Thus, gammacerane has often been used as a proxy from stratification, although care must be taken in interpretation due to the discovery of additional bacterial sources for gammacerane in sediments (Banta et al., 2015).

Prolonged density stratification may be associated with a dominance of prasinophytes, when low-oxygen waters and increased amounts of reduced or regenerated nitrogen reach the lower photic-zone (Prauss, 2007). Prasinophytes are known to become abundant under decreased nitrate and increased ammonium availability (e.g., Cochlan and Harrison, 1991), indicating they were better adapted to the reduced recycling of nutrients that occurs during water column stratification (Prauss,

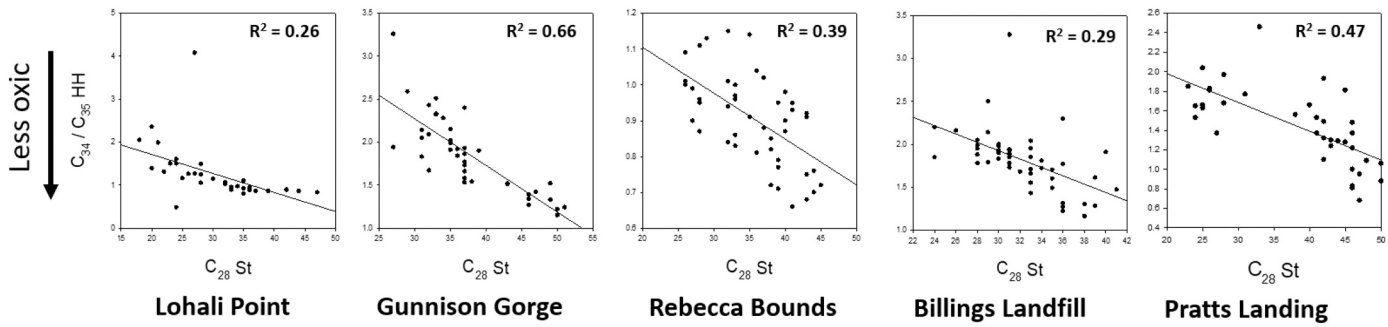

Fig. 11. Cross plots of C_{34}/C_{35} HH (redox) against C_{28} sterane (possible prasinophyte abundance) for all five sites in this study. Please note variation in scale to allow for better visualisation of the site-specific trends.

2007). Prolonged stratification generally favours organisms with a smaller surface area to volume ratio in order to facilitate nutrient uptake, such as nano- or picoplankton (organisms <2 μm; Wells et al., 2015), in which prasinophytes have been shown to be an important component of nano- and pico-plankton in the modern ocean (Litchman et al., 2006).

Boudinot et al. (2020) suggest that prasinophyte abundance in the WIS may be affected by an increase in ammonium N-sources globally during OAE2 (Higgins et al., 2012; Naafs et al., 2019). Whilst this may play an important part in prasinophyte dynamics, data from the Rebecca Bounds core and other WIS studies (Eldrett et al., 2017; Supplemental Material F) show C_{28} steranes and prasinophyte abundance to be higher prior to OAE2 and therefore not affected by any specific OAE2 driven increases in ammonium. We suggest that in the WIS stratification drove reduced nutrient recycling, reduced nitrate availability and, therefore, increased prasinophyte abundance.

3.6. Stratification and anoxia

The proxy for stratification, gammacerane, has relatively high values (up to 0.41; Figs. 12-13) when compared to biotic crises documented from more open ocean settings, such as the end-Triassic mass extinction (~0–0.03: Kasprak et al., 2015), and Toarcian OAE (0.01–0.04, French et al., 2014). Values are more in line with those found during the CTB at other WIS sites, such as west-central Alberta (0.07–0.21: Furmann et al., 2015) and central Texas (up to 0.58: French et al., 2019), alongside those values for lacustrine deposits (0.04–0.42 (Chen and Summons, 2001; Huang et al., 2020; Rizzi et al., 2020; Yin et al., 2020). This suggests that the WIS experienced particularly stratified conditions during the CTB, although local variation exists (e.g., values <0.03 in Utah; Boudinot et al., 2020).

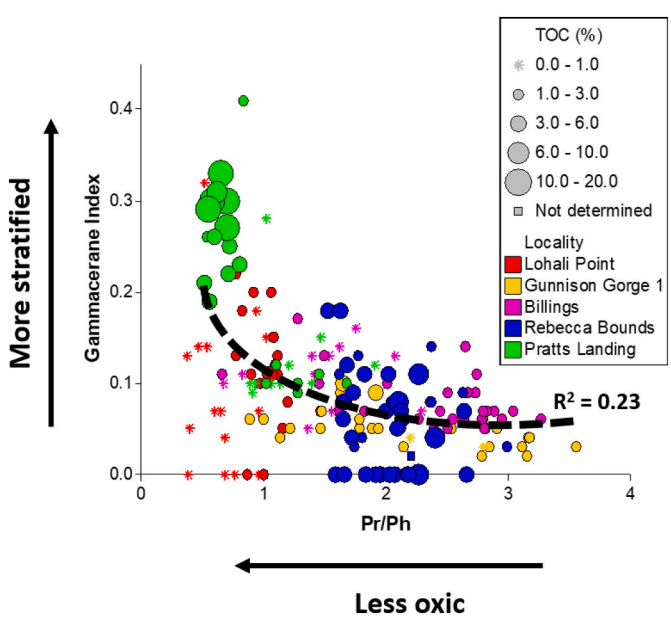

Fig. 12. Crossplot of Gammacerane Index (stratification) and Pr/Ph (redox) for all 5 sites.

In this study stratification generally increases with sea-level (Figs. 3, 4, 7), as increased water depths allowed for a more stable chemocline to develop. The exception to this is at the Rebecca Bounds core, where variability during OAE2 makes trends hard to distinguish, and at Billings Landfill where stratification breaks down during highest sea-levels. The Boreal/Tethyan mixing front is hypothesized to be located close to Billings Landfill during OAE2 (Dameron et al., n.d.) and the effect of associated caballing during high sea-levels at this location may explain the marked decrease in stratification as sea-levels rose.

At all sites, a positive relationship is seen between the stratification proxy, gammacerane, and terrestrial input, particularly at Billings Landfill (Fig. 6) where peaks in oleanane (terrestrial input) correspond closely to peaks in gammacerane. These increases in terrestrial organic matter suggest increased fluvial input, and, whilst increased water-depth is likely to be the main driver of stratification, freshwater-driven salinity stratification may also be an important factor.

In this study, strong stratification is linked to increased anoxia; however, anoxia can also be present in the absence of stratification, particularly in the Lohali Point site (Figs. 3, 12). This is perhaps due to a productivity-driven OMZ rather than a stratified water column (Leckie et al., 1991; Boudinot et al., 2020; Forkner et al., 2021), or due to proxies recording anoxic conditions in the sediments, rather than the overlying water column which was relatively well-mixed and oxygenated (Piper and Calvert, 2009; Plint et al., 2012).

Particularly high sedimentation rates can rapidly bury organic matter on the sea-floor, isolating it from potentially oxidizing bottom waters and causing pore-waters, only a few millimeters below the sea-floor in some instances to become anoxic (Piper and Calvert, 2009; Plint et al., 2012). This model may explain the discrepancies between high benthic faunal abundances and geochemical proxies suggesting anoxia, or at least low oxygen conditions. The BOZ at Billings, represents such a phase, where high sedimentation rates (indicated by a large pulse of terrestrial input at a height of 19–24 m) coincide with a brief interval of slightly increased foraminiferal abundance and geochemical evidence for anoxia (Fig. 6). Lohali Point is another site with high sedimentation where geochemical redox proxies point towards anoxic conditions alongside the presence of benthic foraminifera. Many authors, however, favour the model of intermittent anoxia to explain these discrepancies, where faunal changes and anoxic proxies may be recording different time scales of environmental change (e.g., Simons and Kenig, 2001; Boudinot et al., 2020; Bryant et al., 2021; Forkner et al., 2021). Whilst not likely to be the sole driver for these paradoxical signals, anoxia just below the sediment-water interface is one hypothesis to explain geochemical proxy records of increased anoxia at sites with high

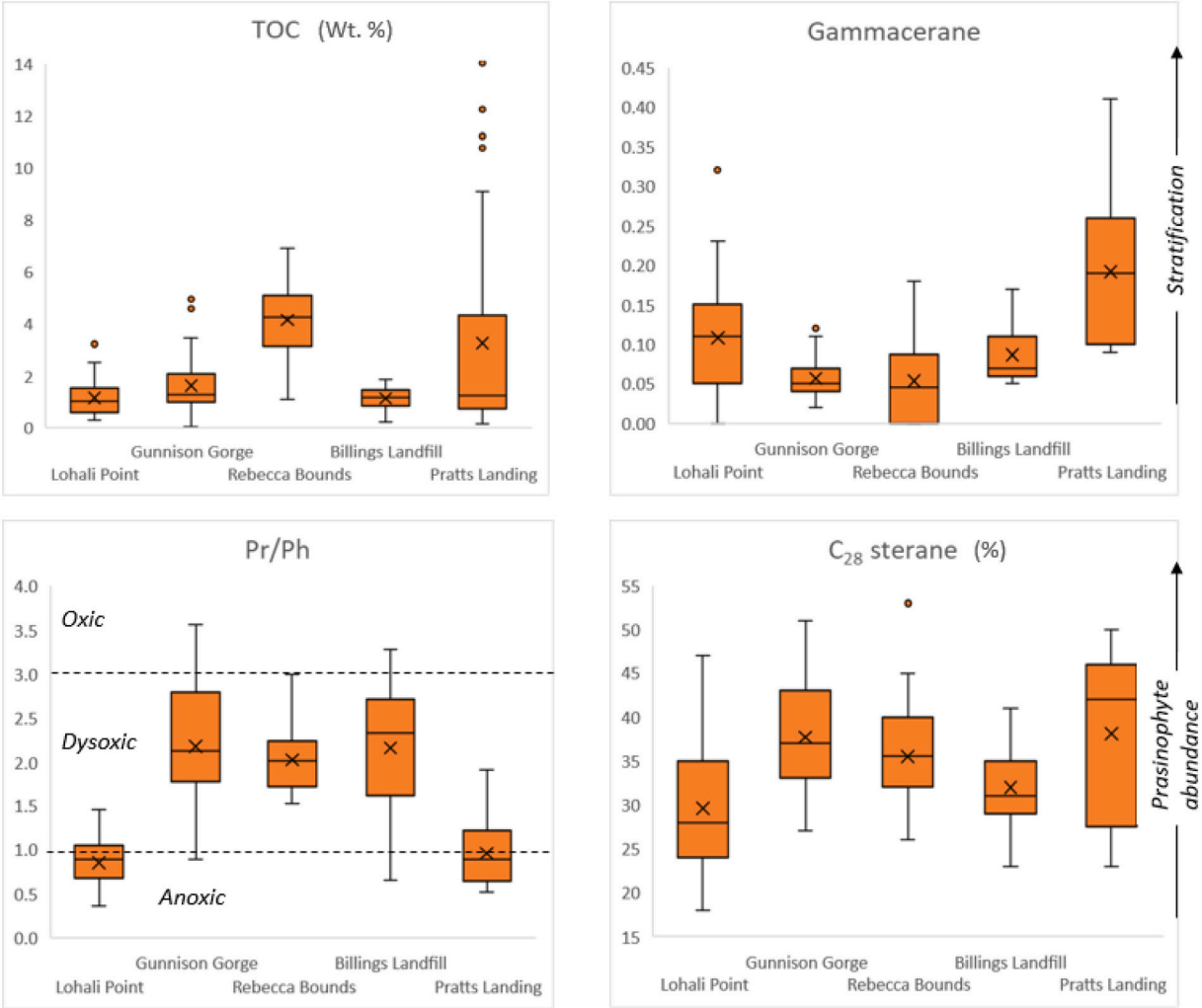

Fig. 13. Box and whisker diagrams showing data distribution for four key oceanographic proxies across all five sites: TOC, Gammacerane (Gammacerane/(gammacerane + C_{30} αβ hopane): stratification proxy), Pristane/Phytane (redox proxy) and C_{28} sterane (C_{28} steranes / $\sum(C_{27-29}$ steranes) * 100: prasinophyte proxy). Line within the box indicates median, cross within the box indicates the mean. See Table 1 for more information on geochemical proxies.

sedimentation rates, especially when geochemical proxies are countered by micropalaeontological indicators.

3.7. Photic zone euxinia (PZE)

Photic zone euxinia (PZE) is a phenomenon whereby anoxia and free hydrogen sulfide extend into the shallow photic zone, and is usually related to particularly strong anoxic conditions extending from the seafloor (Pancost et al., 2004). Isorenieratane, a marker for photic zone euxinia, was difficult to resolve in the chromatogram of the aromatic fraction, suggesting low overall concentrations. As such, a crude assessment of the presence of its derivative molecules was undertaken (see Methods – Lipid biomarkers). These data broadly follow redox trends from Pr/Ph and C_{34}/C_{35} HH for Lohali Point, Rebecca Bounds and Pratts Landing (Figs. 3, 5, 7), suggesting that PZE is linked to stronger anoxic conditions at the sea floor. Gunnison Gorge shows no variation of isorenieratane, however (Fig. 4), and data from Billings Landfill show opposing trends (Fig. 6). Isorenieratane derivatives are absent at Billings Landfill during lowest values of redox proxies (20.5–23 m height), further supporting the hypothesis of anoxic pore waters underneath an otherwise mixed and oxygenated water column. Other studies on CTB sections have noted isorenieratane derivatives within bioturbated limestone beds across the central US WIS (Simons and Kenig, 2001), and in sediments containing benthic and planktic foraminifera in southern Utah (Boudinot et al., 2020). These studies have postulated that PZE alongside faunal activity highlights the dynamic nature of redox conditions in the WIS, where intermittent anoxic events can alternate with intervals of increased oxygenation and may indicate seasonal, or other episodic, drivers of redox conditions (Boudinot et al., 2020; Forkner et al., 2021). All samples are composites of environments across a range of time, indicating the need for future studies at sedimentary lamination level.

Our data support low isorenieratane concentrations in all studied sections and indicate no prominent episodes of PZE. This contrasts with Boudinot et al. (2020) who propose that elevated isorenieratane and an increase in anoxia during OAE2 at the SH#1 core in Utah is due to the site's unique depositional environment along the productive western margin. Although this core is only 180 km from Lohali Point in present-day geography, during the CTB they do not exhibit similar trends in terrigenous input, stratification or redox, suggesting terrestrial influence, palaeobathymetry and oceanography may have been very different between these two sites along the western margin of the WIS.

Based on isorenieratane presence, Simons et al. (2003) suggested a more dynamic and well-mixed southern WIS compared to the less-oxygenated Canadian part of the basin. Whilst our data do not show elevated isorenieratane within the northern Pratts Landing section, elevated gammacerane and TOC coupled with decreased Pr/Ph and C_{34}/C_{35} HH do suggest a well-stratified, anoxic environment (Fig. 7).

3.8. Benthonic zone (BOZ)

The BOZ has been identified by increased abundances of planktic and benthic foraminifera in the *Sciponoceras* biozone of Lohali Point (Leckie et al., 1998; West et al., 1998) and Billings Landfill (Dameron et al., n.d.). Lowery et al. (2018) propose that increased oxygen was the primary control on foraminifera abundance in the WIS, ruling out the effects of salinity, pH and water depth. Redox proxy data within this study, however, do not conclusively support oxygenation during the BOZ for these sites. This may be due to high sedimentation rates at these sites driving increased pore-water anoxia, but the limited nature of the BOZ at these sites compared to those more central in the seaway does also point to generally inhospitable conditions in the proximal realm, perhaps related to productivity-driven expansion of the OMZ (Leckie et al., 1998; Dameron et al., n.d.). While these findings are in agreement with that of another proximal site in Utah (Boudinot et al., 2020), where no increase in oxygenation is apparent during OAE2, they contradict those of Lowery et al. (2018) who find increased benthic foraminiferal abundances along the western proximal part of the basin. Foraminiferal analysis has not been conducted at Pratts Landing, however, despite trace amounts of planktic foraminifera in the Belle Fouche Formation of Alberta, Saskatchewan and Manitoba (McNeil and Caldwell, 1981; Bloch et al., 1999), the BOZ is not generally recognised at significant levels in Canadian sites.

Whilst redox proxies are not necessarily an optimal marker for the BOZ, this study shows that sterane abundance may be a more useful marker. At Lohali Point, Billings Landfill and Rebecca Bounds, the onset of the CIE (i.e., equivalent to the timing of the BOZ) is marked by a minima in C_{28} sterane values (Figs. 3, 5, 6). Furthermore, an assessment of published sterane data across the WIS shows a decrease in C_{28} sterane, or generally low values, within OAE2 is common at sites across Texas, New Mexico and Colorado (Supplemental Material F). This supports the presence of more habitable 'normal marine' waters during the BOZ without the high abundances of prasinophytes that characterise much of the CTB.

3.9. Comparison of sites

This study of five sites shows clear heterogeneity in terms of geochemical expressions of oceanography, redox conditions and ecological change across the WIS (Fig. 13):

- Lohali Point exhibits some of the lowest, and most anoxic, redox values, yet is characterised by low prasinophyte occurrence and organic matter preservation, and diverse foraminiferal assemblages (Leckie et al., 1991). We suggest this disparity is due to particularly high sedimentation rates, enhancing burial of sediments and causing pore-waters to become anoxic, a hypothesis supported by studies of proximal sites in the Canadian WIS (Plint et al., 2012). Thus geochemical signals are enhanced by pore-water anoxia, rather than reflecting the true redox state of the water column.
- The Gunnison Gorge section does not include the CIE of OAE2 due to its location on a bathymetric high and subsequent winnowing of any sediments that may have been depsotied during OAE2. The low water depths of this section are expressed by redox values suggesting a relatively oxygenated environemnt, with low organic matter accumulation and low TOC values.
- The most distal site here, Rebecca Bounds, has the highest levels of organic matter accumulation due its distance from clastic sediment input that would otherwise dilute organic matter.
- An oceanographic front is postulated at the Billings Landfill site, due to the decrease in stratification concurrent with an increase in water depth. This is counter to trends seen in other proximal sites in basin and suggests caballing, or at least increased water column overturning, at this site during highest sea-levels indicative of a mixing between two water masses.
- Pratts Landing is the most northerly site and exhibits vastly different trends to other sites studied here, with particularly high TOC values and geochemical proxies suggestive of very stratified, anoxic and prasinophyte-rich waters from sediments deposited during OAE2 and beyond. This difference in geochemical signal suggests a vastly different oceanographic regime, and further supports the presence of a Boreal-Tethyan oceanographic front between Canada and the US – potentially in the proximity of the Billings Landfill site.

4. Conclusions

Environmental conditions across the mid-Cretaceous OAE2 within the five sites studied here (Lohali Point, Gunnison Gorge, Rebecca Bounds, Billings Landfill and Pratts Landing) show clear differences, indicating heterogeneity and complexity in the drivers resulting in anoxia, stratification and organic matter deposition across the basin.

Despite these differences, trends among geochemical proxies can be demonstrated. At most sites (Lohali Point, Gunnison Gorge and Pratts Landing) stratification appears to lead to low-oxygen conditions, driven by increased water depths allowing a more stable chemocline to develop. In addition to water depth, stratification can be locally enhanced by increases in low-density freshwater run-off in the upper water column. At Billings Landfill, however, a breakdown in stratification occurred as water depths increased, suggesting caballing and the local presence of the mixing front between Boreal and Tethyan waters.

The C_{28} sterane is shown to be a useful proxy for presence of prasinophyte algae. Prasinophyte-rich algal productivity is evident at every site, driven by increased stratification and possibly linked to perturbations of the marine biogeochemical cycle, such as the increase of ammonium nitrogen sources.

Evidence for prasinophyte dominance decreases at the onset of OAE2 for sites within the US part of the WIS, concurrent with the presence of the BOZ. An increase in oxygenation is not always identified at the BOZ in proximal sites, due to the influence of high rates of terrigenous sedimentation, pore-water anoxia and/or enhanced nutrient-driven productivity. We show that sterane ratios are a more reliable geochemical proxy for assessing changes in faunal communities and identifying the presence of the BOZ.

Intermittent dysoxia/oxic conditions allowed benthos to exist on the sea floor, in some cases in beds that contain evidence for anoxia and PZE. In addition to this, we propose that pore-water anoxia, occurring where there is particularly high sedimentation rates along the western part of the WIS, can enhance the anoxic signal in sediments accumulating beneath a well-oxygenated water column. As a result, proximal sites show differing trends relative to the more centrally located Rebecca Bounds core.

This study is one example of how a multidisciplinary approach based on several different indicators and proxies can facilitate the disentanglement of seemingly conflicting data sets, leading to a more robust assessment of environmental conditions captured in ancient sediments across extreme episodes.

Author contributions

LJR and JHW designed the study; LJR, JL and SM logged and obtained samples for Gunnison Gorge; LJR and KSG generated isotopic, elemental, lipid biomarker and palynofacies data; ICH and JEAM assisted with palynological preparation and interpretation; PB generated nannofossil data; CPF conducted PCA statistics. DRG generated isotopic data, and NAGMvH and NMP generated palynofacies data, for Pratts Landing. RML provided samples for Lohali Point and Billings Landfill and contributed valuable scientific input, SD provided analysis for the Billings Landfill site. LJR and JHW wrote the manuscript with, input from all co-authors.

Declaration of Competing Interest

The authors declare that they have no known competing financial interests or personal relationships that could have appeared to influence the work reported in this paper.

Data availability

Robinson et al C/T organic geochem data from five sites in the Western Interior Seaway (Original data) (Mendeley Data)

Acknowledgements

LJR acknowledges support from the Natural Environmental Research Council UK (NE/L002531/1), AAPG Foundation Grant-in-Aid (Marta S. Weeks Named Grant) and Geological Society of London Research Grant (William George Fearnsides fund). Samples were generously donated by Mark Leckie (Lohali Point and Billings Landfill), Guy Plint (Pratts Landing) and the USGS Core Research Centre (Rebecca Bounds). Samples from Lohali Point originate from Navajo and Hopi ancestral lands. We thank the Bureau of Land Management for access to Gunnison Gorge NCA, with work conducted under BLM permit to JRL. Marjean Cone assisted in sample acquisition from Gunnison Gorge, and David Noe provided important guidance on the stratigraphy of the area. We thank Richard Twitchett (Natural History Museum) for insightful conversations. CPF acknowledges CIRA grant CIRA-2019-066.

Appendix A. Supplementary data

Supplementary data to this article can be found online at https://doi.org/10.1016/j.palaeo.2023.111496.

References

Adams, D.D., Hurtgen, M.T., Sageman, B.B., 2010. Volcanic activation of biogeochemical cascade regulates Oceanic Anoxic Event 2. Geochimica Et Cosmochimica Acta Conference on Goldschmidt 2010 - Earth, Energy, and the Environment 74 (12).

Allison, P., Wells, M., 2006. Circulation in large ancient epicontinental seas: what was different and why? Palaios 21, 513–515.

Arthur, M.A., Sageman, B.B., 2005. Sea Level Control on Source Rock Development: Perspectives from the Holocene Black Sea, the mid-Cretaceous Western Interior Basin of North America, and the Late Devonian Appalachian Basin. In: Harris, N.B. (Ed.), The Deposition of Organic Carbon-Rich Sediments: Models. Mechanisms and Consequences, SEPM.

Arthur, M.A., Schlanger, S.O., Jenkyns, H.C., 1987. The Cenomanian-Turonian Oceanic Anoxic Event, II. Palaeoceanographic controls on organic matter production and preservation. Geological Society, London, Special Publications 26 (1), 401–420.

Banta, A.B., Wei, J.H., Welander, P.V., 2015. A distinct pathway for tetrahymanol synthesis in bacteria. Proc. Nat. Acad. Sci. 112, 13478–13483.

Baranyi, V., Pálfy, J., Görög, Á., Riding, J.B., Raucsik, B., 2016. Multiphase response of palynomorphs to the Toarcian Oceanic Anoxic Event (Early Jurassic) in the Réka Valley section, Hungary. Rev. Palaeobot. Palynol. 235, 51–70.

Barnosky, A.D., Matzke, N., Tomiya, S., Wogan, G.O.U., Swartz, B., Quental, T.B., Marshall, C., McGuire, J.L., Lindsey, E.L., Maguire, K.C., Mersey, B., Ferrer, E.A., 2011. Has the Earth's sixth mass extinction already arrived? Nature 471, 51–57.

Bhattacharya, J.P., Tye, R.S., 2004. Searching for Modern Ferron Analogs and Application to Subsurface Interpretation. https://doi.org/10.1306/St50983.

Bloch, J.D., Schröder-Adams, C.J., Leckie, D.A., Craig, J., McIntyre, D.J., 1999. Sedimentology, micropalaeontology, geochemistry and hydrocarbon potential of shale from the cretaceous lower Colorado group in Western Canada (No. 531), Geological Survey of Canada, Bulletin.

Boudinot, F.G., Dildar, N., Leckie, R.M., Parker, A., Jones, M.M., Sageman, B.B., Bralower, T.J., Sepúlveda, J., 2020. Neritic ecosystem response to Oceanic Anoxic Event 2 in the Cretaceous Western Interior Seaway, USA. Palaeogeogr. Palaeoclimatol. Palaeoecol. 546, 109673.

Bralower, T.J., Bergen, J.A., 1998. Cenomanian-Santonian Calcareous Nannofossil Biostratigraphy of a Transect of Cores Drilled Across the Western Interior Seaway. https://doi.org/10.2110/csp.98.06.0059.

Breitburg, D., Levin, L.A., Oschlies, A., Grégoire, M., Chavez, F.P., Conley, D.J., Garçon, V., Gilbert, D., Gutiérrez, D., Isensee, K., Jacinto, G.S., Limburg, K.E., Montes, I., Naqvi, S.W.A., Pitcher, G.C., Rabalais, N.N., Roman, M.R., Rose, K.A., Seibel, B.A., Telszewski, M., Yasuhara, M., Zhang, J., 2018. Declining oxygen in the global ocean and coastal waters. Science 359, eaam7240.

Brocks, J.J., Jarrett, A.J.M., Sirantoine, E., Hallmann, C., Hoshino, Y., Liyanage, T., 2017. The rise of algae in Cryogenian oceans and the emergence of animals. Nature 548, 578–581.

Bryant, R., Leckie, M.R., Bralower, T.J., Jones, M.M., Sageman, B.B., 2021. Microfossil and geochemical records reveal high-productivity palaeoenvironments in the cretaceous Western Interior Seaway during Oceanic Anoxic Event 2. Palaeogeogr. Palaeoclimatol. Palaeoecol. 584, 110679 https://doi.org/10.1016/j.palaeo.2021.110679.

Caldwell, W.G.E., Diner, R., Eicher, D.G., Fowler, S.P., North, B.R., Stelck, C.R., von Holdt Wilhelm, L., 1993. Foraminiferal biostratigraphy of Cretaceous marine cyclothems. In: Caldwell, W.G.E., Kauffman, E.G. (Eds.), Evolution of the Western Interior Basin. Geological Association of Canada, pp. 477–520.

Ceballos, G., Ehrlich, P.R., Dirzo, R., 2017. Biological annihilation via the ongoing sixth mass extinction signaled by vertebrate population losses and declines. Proc. Nat. Acad. Sci. 114. E6089–E6096.

Chen, J., Summons, R.E., 2001. Complex patterns of steroidal biomarkers in Tertiary lacustrine sediments of the Biyang Basin, China. Org. Geochem. 32 (1), 115–126.

Cobban, W.A., Scott, G.R., 1972. Stratigraphy and ammonite fauna of the Graneros Shale and Greenhorn Limestone near Pueblo, Colorado. Colorado Geological Survey Profession Paper, p. 645.

Cochlan, W., Harrison, P., 1991. Uptake of nitrate, ammonium, and urea by nitrogen-starved cultures of Micromonas pusilla (Prasinophyceae): Transient responses. J. Phycol. 27, 673–679.

Cronin, S.J., Neall, V.E., Lecointre, J.A., Hedley, M.J., Loganathan, P., 2003. Environmental hazards of fluoride in volcanic ash: a case study from Ruapehu volcano, New Zealand. J. Volcanol. Geotherm. Res. 121, 271–291.

Curiale, J.A., 1994. Geochemical anomalies at the Cenomanian-Turonian Boundary, Northwest New-Mexico. Org. Geochem. 22, 487–500.

Dameron, S.N., Leckie, R.M., Polyak, D.E., Robinson, L.J., Whiteside, J.H., Elder, W.P., Leithold, E.L., Tibert, N.E., In Review. A Palaeoceanographic Divide in the Western Interior Seaway during the Cenomanian-Turonian OAE2. Micropalaeontology.

Dickson, A.J., Jenkyns, H.C., Porcelli, D., van den Boorn, S., Idiz, E., 2016a. Basin-scale controls on the molybdenum-isotope composition of seawater during Oceanic Anoxic Event 2 (Late Cretaceous). Geochim. Cosmochim. Acta 178, 291–306.

Dickson, A.J., Jenkyns, H.C., Porcelli, D., van den Boorn, S., Idiz, E., Owens, J.D., 2016b. Corrigendum to "Basin-scale controls on the molybdenum-isotope composition of seawater during Oceanic Anoxic Event 2 (Late Cretaceous)" [Geochim. Cosmochim. Acta 178 (2016) 291–306]. Geochim. Cosmochim. Acta 189, 404–405.

Didyk, B.M., Simoneit, B.R.T., Brassell, S.C., Eglinton, G., 1978. Organic geochemical indicators of palaeo-environmental conditions of sedimentation. Nature 272, 216–222.

Dionne, D., Schroder-Adams, C., Cumbaa, S., 2016. Foraminiferal response to Ecological perturbations along the eastern margin of the Canadian Western Interior seaway, Cenomanian-Turonian interval. J.Foraminiferal Res. 46, 124–148.

Dirzo, R., Young, H.S., Galetti, M., Ceballos, G., Isaac, N.J.B., Collen, B., 2014. Defaunation in the Anthropocene. Science 345, 401–406.

Dougherty, R.C., Strain, H.H., Svec, W.A., Uphaus, R.A., Katz, J.J., 1970. Structure, properties, and distribution of chlorophyll c. J. Am. Chem. Soc. 92, 2826–2833.

Du Vivier, A.D.C., Selby, D., Sageman, B.B., Jarvis, I., Gröcke, D.R., Voigt, S., 2014. Marine 187Os/188Os isotope stratigraphy reveals the interaction of volcanism and ocean circulation during Oceanic Anoxic Event 2. Earth Planet.Sci.Lett. 389, 23–33. https://doi.org/10.1016/j.epsl.2013.12.024.

Eglinton, T.I., Eglinton, G., 2008. Molecular proxies for paleoclimatology. Earth Planet. Sci. Lett. 275 (1), 1–16. https://doi.org/10.1016/j.epsl.2008.07.012.

Eicher, D.L., Diner, R., 1985. Foraminifera as Indicators of Water Mass in the Cretaceous Greenhorn Sea, Western Interior. In: Pratt, L.M., Kauffman, E.G., Zelt, F.B. (Eds.), Fine-Grained Deposits and Biofacies of the Cretaceous Western Interior Seaway. SEPM Society for Sedimentary Geology, Tulsa, OK, pp. 60–71.

Eicher, D.L., Worstell, P., 1970. Cenomanian and Turonian Foraminifera from the Great Plains, United States. Micropalaeontology 16, 269–324.

Elder, W.P., Kirkland, J.I., 1985. Stratigraphy and Depositional Environments of the Bridge Creek Limestone Member of the Greenhorn Limestone at Rock Canyon Anticline Near Pueblo, Colorado. In: Fine-Grained Deposits and Biofacies of the Cretaceous Western Interior Seaway: Evidence of Cyclic Sedimentary Processes, SEPM Field Trip Guide 4. https://doi.org/10.2110/sepmfg.04.122.

Elder, W.P., 1987. The Palaeoecology of the Cenomanian-Turonian (Cretaceous) Stage Boundary Extinctions at Black Mesa, Arizona. Palaios 2, 24–40.

Elderbak, K., Leckie, R.M., 2016. Palaeocirculation and foraminiferal assemblages of the Cenomanian-Turonian Bridge Creek Limestone bedding couplets: productivity vs. dilution during OAE2. Cretac. Res. 60, 52–77.

Elderbak, K., Leckie, R.M., Tibert, N.E., 2014. Palaeoenvironmental and palaeoceanographic changes across the Cenomanian-Turonian Boundary Event (Oceanic Anoxic Event 2) as indicated by foraminiferal assemblages from the eastern margin of the Cretaceous Western Interior Sea. Palaeogeogr. Palaeoclimatol. Palaeoecol. 413, 29–48.

Eldrett, J.S., Dodsworth, P., Bergman, S.C., Wright, M., Minisini, D., 2017. Water-mass evolution in the cretaceous Western Interior Seaway of North America and equatorial Atlantic. Clim. Past 13, 855–878.

Eldrett, J.S., Minisini, D., Bergman, S.C., 2014. Decoupling of the carbon cycle during Ocean Anoxic Event 2. Geology 42, 567–570.

Erbacher, J., Huber, B.T., Norris, R.D., Markey, M., 2001. Increased thermohaline stratification as a possible cause for an ocean anoxic event in the cretaceous period. Nature 409, 325–327.

Falkowski, P.G., Katz, M.E., Knoll, A.H., Quigg, A., Raven, J.A., Schofield, O., Taylo, F.J. R., 2004. The evolution of modern eukaryotic phytoplankto. Science 305 (5682), 354–360. https://doi.org/10.1126/science.1095964.

Fisher, C.G., Hay, W.W., Eicher, D.L., 1994. Oceanic Front in the Greenhorn Sea (Late Middle through late Cenomanian). Palaeoceanography 9, 879–892.
Floegel, S., Hay, W.W., DeConto, R.M., Balukhovsk, A.N., 2005. Formation of sedimentary bedding couplets in the Western Interior Seaway of North America - implications from climate system modeling. Palaeogeogr. Palaeoclimatol. Palaeoecol. 218, 125–143.
Forkner, R.M., Dahl, J., Fildani, A., Barbanti, S.M., Yurchenko, I.A., Moldowan, J.M., 2021. Anatomy of an extinction revealed by molecular fossils spanning OAE2. Sci. Rep. 11, 13621.
French, K.L., Birdwell, J.E., Whidden, K.J., 2019. Geochemistry of a thermally immature Eagle Ford Group drill core in Central Texas. Org. Geochem. 131, 19–33.
French, K.L., Sepúlveda, J., Trabucho-Alexandre, J., Gröcke, D.R., Summons, R.E., 2014. Organic geochemistry of the early Toarcian oceanic anoxic event in Hawsker Bottoms, Yorkshire, England. Earth Planet. Sci. Lett. 390, 116–127.
Furmann, A., Mastalerz, M., Brassell, S.C., Pedersen, P.K., Zajac, N.A., Schimmelmann, A., 2015. Organic matter geochemistry and petrography of Late Cretaceous (Cenomanian-Turonian) organic-rich shales from the Belle Fourche and Second White Specks formations, west-Central Alberta, Canada. Org. Geochem. 85, 102–120.
Gale, A.S., Voigt, S., Sageman, B.B., Kennedy, W.J., 2008. Eustatic sea-level record for the Cenomanian (Late Cretaceous)—extension to the Western Interior Basin, USA. Geology 36, 859.
Grice, K., Schaeffer, P., Schwark, L., Maxwell, J.R., 1996. Molecular indicators of palaeoenvironmental conditions in an immature Permian shale (Kupferschiefer, Lower Rhine Basin, north-west Germany) from free and S-bound lipids. Organic Geochemistry 25 (3/4), 131–147.
Hancock, J.M., Kauffman, E.G., 1979. The great transgressions of the Late Cretaceous. J. Geol. Soc. 136, 175–186.
Hattin, D.E., 1985. Distribution and Significance of Widespread, Time-Parallel Pelagic Limestone Beds in Greenhorn Limestone (Upper Cretaceous) of the Central Great Plains and Southern Rocky Mountains. In: Fine-Grained Deposits and Biofacies of the Cretaceous Western Interior Seaway: Evidence of Cyclic Sedimentary Processes, SEPM Field Trip Guide 4. https://doi.org/10.2110/sepmfg.04.028.
Hawkins, E., Ortega, P., Suckling, E., Schurer, A., Hegerl, G., Jones, P., Joshi, M., Osborn, T.J., Masson-Delmotte, V., Mignot, J., Thorne, P., van Oldenborgh, G.J., 2017. Estimating changes in global temperature since the preindustrial period. Bull. Am. Meteorol. Soc. 98, 1841–1856.
Hay, W.W., Flögel, S., 2012. New thoughts about the Cretaceous climate and oceans. Earth-Sci. Rev. 115 (4), 262–272. https://doi.org/10.1016/j.earscirev.2012.09.008.
Hay, M.J., Plint, A.G., 2020. High-frequency sequences within a retrogradational deltaic succession: Upper Cenomanian Dunvegan Formation, Western Canada Foreland Basin. The Depositional Record 6, 524–551.
Hay, W.W., Eicher, D., Diner, L., 1993. Physical oceanography and water masses of the Cretaceous Western Interior Seaway. In: Caldwell, W.G.E., Kauffman, E.G. (Eds.), Evolution of the Western Interior Basin. Geological Association of Canada, pp. 297–318.
Higgins, M.B., Robinson, R.S., Husson, J.M., Carter, S.J., Pearson, A., 2012. Dominant eukaryotic export production during ocean anoxic events reflects the importance of recycled NH4+. Proc. Nat. Acad. Sci. 109, 2269–2274.
Huang, W.Y., Meinschein, W.G., 1979. Sterols as ecological indicators. Geochimica Et Cosmochimica Acta 43 (5), 739–745.
Huang, S., Xu, G., Xu, F., Wang, W., Yuan, H., Yan, Z., Lin, X., Zhang, M., 2020. Biomarker distributions and depositional environments of continental source rocks in Sichuan Basin, SW China. Energy Exploration & Exploitation 38 (6), 1–29. https://doi.org/10.1177/01445987209155.
Ipcc, 2021. Climate Change 2021: the Physical Science Basis. In: Contribution of Working Group I to the Sixth Assessment Report of the Intergovernmental Panel on Climate Change. Cambridge University Press.
Jarvis, I., Lignum, J.S., Gröcke, D.R., Jenkyns, H.C., Pearce, M.A., 2011. Black shale deposition, atmospheric CO2 drawdown and cooling during the Cenomanian-Turonian Oceanic Anoxic Event. Palaeoceanography 26, PA3201. https://doi.org/10.1029/2010PA002081.
Jenkyns, H.C., 1980. Cretaceous anoxic events: from continents to oceans. J. Geol. Soc. 137, 171–188.
Jenkyns, H.C., 2003. Evidence for rapid climate change in the Mesozoic-Palaeogene greenhouse world. Philosophical Transactions of the Royal Society a-Mathematical Physical and Engineering Sciences 361, 1885–1916.
Jenkyns, H.C., 2010. Geochemistry of oceanic anoxic events. Geochemistry Geophysics Geosystems 11. Artn Q03004 10.1029/2009gc002788.
Joo, Y.J., Sageman, B.B., 2014. Cenomanian to Campanian Carbon Isotope Chemostratigraphy from the Western Interior Basin, USA. J. Sediment. Res. 84, 529–542.
Kasprak, A.H, Sepúlveda, J., Price-Waldman, R., Williford, K.H., Schoepfer, S.D., Haggart, J.W., Ward, P.D., Summons, R.E., Whiteside, J.H., 2015. Episodic photic zone euxinia in the northeastern Panthalassic Ocean during the end-Triassic extinction. Geology 43 (4), 307–310.
Kauffman, E.G., 1984. Palaeobiogeography and evolutionary response dynamic in the Cretaceous Western Interior Seaway of North America. In: Westerman, G.E.G. (Ed.), Jurassic-Cretaceous Biochronology and Palaeogeography of North America. Geological Association of Canada, pp. 273–306.
Kauffman, W.G.E., Caldwell, W.G., 1993. The Western Interior Basin in Space and Time. In: Evolution of the Western Interior Basin. Geological Association of Canada, pp. 1–30.
Keeling, R.E., Körtzinger, A., Gruber, N., 2010. Ocean deoxygenation in a warming world. Annu. Rev. Mar. Sci. 2, 199–229.
Keller, G., Pardo, A., 2004. Age and palaeoenvironment of the Cenornanian-Turonian global stratotype section and point at Pueblo, Colorado. Marine Micropalaeontol. 51, 95–128.
Kennedy, W.J., Walaszczyk, I., Cobban, W.A., 2005. The Global Boundary Stratotype Section and Point for the base of the Turonian Stage of the Cretaceous: Pueblo, Colorado, U.S.A. Episodes 28 (2), 93–104.
Kidder, D.L., Worsley, T.R., 2010. Phanerozoic large Igneous Provinces (LIPs), HEATT (Haline Euxinic Acidic thermal Transgression) episodes, and mass extinctions. Palaeogeogr. Palaeoclimatol. Palaeoecol. 295, 162–191.
Kirkland, J.I., 1991. Lithostratigraphic and biostratigraphic framework for hte Mancos Shale (Late Cenomanian to Middle Turonian) at Black Mesa, northeastern Arizona. In: Nations, J.G., J.D., . Eaton (Eds.), Stratigraphy, Depositional Environments, and Sedimentary Tectonics of the Western Margin, Cretaceous Western Interior Seaway. Geological Society of America.
Kirkland, J.I., 1996. Palaeontology of the Greenhorn cyclothem (Cretaceous: Late Cenomanian to Middle Turonian) at Black Mesa, northeastern Arizona. New Mexico Museum of Natural History.
Knoll, A.H., Summons, R.E., Waldbauer, J.R., Zumberge, J.E., 2007. The Geological Succession of Primary Producers in the Oceans. In: Evolution of Primary Producers in the Sea, pp. 133–163.
Kodner, R.B., Pearson, A., Summons, R.E., Knoll, A.H., 2008. Sterols in red and green algae: quan-tification, phylogeny, and relevance for the interpretation of geologic steranes. Geobiology 6, 411–420.
Kump, L.R., Slingerland, R.L., 1999. Circulation and stratification of the early Turonian Western Interior Seaway: sensitivity to a variety of forcings. In: Evolution of the Cretaceous Ocean-Climate System. Geological Society of America. https://doi.org/10.1130/0-8137-2332-9.181.
Kuroda, J., Ogawa, N.O., Tanimizu, M., Coffin, M.F., Tokuyama, H., Kitazato, H., Ohkouchi, N., 2007. Contemporaneous massive subaerial volcanism and late cretaceous Oceanic Anoxic Event 2. Earth Planet. Sci. Lett. 256, 211–223.
Leckie, R.M., Bralower, T.J., Cashman, R., 2002. Oceanic anoxic events and plankton evolution: biotic response to tectonic forcing during the mid-cretaceous. Palaeoceanography 17. Artn 1041 10.1029/2001pa000623.
Leckie, R.M., Schmidt, M.G., Finkelstein, D., Yuretich, R., 1991. Palaeoceanographic and palaeoclimatic interpretations of the Mancos Shale (Upper Cretaceous), Black Mesa Basin, Arizona. In: Nations, J.G. (Ed.), Stratigraphy, Depositional Environments, and Sedimentary Tectonics of the Western Margin, Cretaceous Western Interior Seaway, Special Paper 260. Geological Society of America, pp. 139–152.
Leckie, R.M., Yuretich, R.F., West, O.L.O., Finkelstein, D., Schmidt, M., 1998. In: Dean, W.E., Arthur, M.A. (Eds.), Stratigraphy and Palaeoenvironments of the Cretaceous Western Interior Seaway, USA. SEPM (Society for Sedimentary Geology). https://doi.org/10.2110/csp.98.06.
Li, R.W., 1989. Geological occurrence and its palaeoenvironmental significance of gammacerane. Chin. Sci. Bull. 34, 1208–1211.
Li, Z., Bhattacharya, J., Schieber, J., 2015. Evaluating along-strike variation using thin-bedded facies analysis, Upper Cretaceous Ferron Notom Delta, Utah. Sedimentology 62, 2060–2089.
Litchman, E., Klausmeier, C.A., Miller, J.R., Schofield, O.M., Falkowski, P.G., 2006. Multi-nutrient, multi-group model of present and future oceanic phytoplankton communities 22.
Lowery, C.M., Leckie, R.M., Bryant, R., Elderbak, K., Parker, A., Polyak, D.E., Schmidt, M., Snoeyenbos-West, O., Sterzinar, E., 2018. The Late Cretaceous Western Interior Seaway as a model for oxygenation change in epicontinental restricted basins. Earth Sci. Rev. 177, 545–564.
Lockshin, S.N., Yacobucci, M.M., Gorsevski, P., Gregory, A., 2017. Spatial characterization of Cretaceous Western Interior Seaway paleoceanography using foraminifera, fuzzy sets and Dempster-Shafer theory. GeoResJ 14, 98–120.
Lowery, Cunningham, R., Barrie, C.D., Bralower, T., Snedden, J.W., 2017. The Northern Gulf of Mexico during OAE2 and the relationship between water depth and Black Shale development. Palaeoceanography 32, 1316–1335.
Mackenzie, A.S., Patience, R.L., Maxwell, J.R., Vandenbroucke, M., Durand, B., 1980. Molecular Parameters of Maturation in a Toarcian Shales, Paris Basin, France-I. Changes in the Configuration of Acyclic Isoprenoid Alknes, Steranes, and Triterpanes. Geochimica et Cosmochimica Acta 44, 1709–1721. https://doi.org/10.1016/0016-7037(80)90222-7.
McNeil, D.H., Caldwell, W.G.E., 1981. Cretaceous Rocks and their Foraminifera in the Manitoba Escarpment, the Geological Association of Canada special Paper 21. The Geological Association Of Canada.
Moldowan, J.M., Dahl, J., Huizinga, B.J., Fago, F.J., Hickey, L.J., Peakman, T.M., Taylor, D.W., 1994. The molecular fossil record of oleanane and its relation to angiosperms. Science 265, 768–771.
Monteiro, F.M., Pancost, R.D., Ridgwell, A., Donnadieu, Y., 2012. Nutrients as the dominant control on the spread of anoxia and euxinia across the Cenomanian-Turonian oceanic anoxic event (OAE2): model-data comparison. Palaeoceanography 27. https://doi.org/10.1029/2012PA002351.
Naafs, B.D.A., Monteiro, F.M., Pearson, A., Higgins, M.B., Pancost, R.D., Ridgwell, A., 2019. Fundamentally different global marine nitrogen cycling in response to severe ocean deoxygenation. Proc. Nat. Acad. Sci. 116, 24979–24984.
Noe, D.C., 2015. Geologic map of the Paonia Quadrangle Delta County, Colorado. Author's Notes. Colorado Geological Survey Open File Report 15-07.
O'Brien, C.L., Robinson, S.A., Pancost, R.D., Damste, J.S.S., Schouten, S., Lunt, D.J., Alsenz, H., Bomemann, A., Bottini, C., Brassell, S.C., Farnsworth, A., Forster, A., Huber, B.T., Inglis, G.N., Jenkyns, H.C., Linnert, C., Littler, K., Markwick, P., McAnena, A., Mutterlose, J., Naafs, B.D.A., Puttmann, W., Sluijs, A., van Helmond, N.A.G.M., Vellekoop, J., Wagner, T., Wrobel, N.E., 2017. Cretaceous sea-

surface temperature evolution: constraints from TEX86 and planktonic foraminiferal oxygen isotopes. Earth Sci. Rev. 172, 224–247.
Ostrander, C.M., Owens, J.D., Nielsen, S.G., 2017. Constraining the rate of oceanic deoxygenation leading up to a Cretaceous Oceanic Anoxic Event (OAE2: ~94 Ma). Sci. Adv. 3, e1701020.
Ourisson, G., Albrecht, P., Rohmer, M., 1979. The Hopanoids: Palaeochemistry and biochemistry of a group of natural products. Pure. Appl. Chem. 51, 709–729.
Owens, J.D., Gill, B.C., Jenkyns, H.C., Bates, S.M., Severmann, S., Kuypers, M.M.M., Woodfine, R.G., Lyons, T.W., 2013. Sulfur isotopes track the global extent and dynamics of euxinia during Cretaceous Oceanic Anoxic Event 2. Proc. Nat. Acad. Sci. 110, 18407–18412.
Pancost, M.A., Freeman, K.H., Arthur, M.A., 1998. Organic geochemistry of the Cretaceous Western Interior Seaway: a trans-basinal evaluation. In: SEPM Concepts in Sedimentology and Palaeontology, 6, pp. 173–188.
Pancost, R.D., Crawford, N., Magness, S., Turner, A., Jenkyns, H.C., Maxwell, J.R., 2004. Further evidence for the development of photic-zone euxinic conditions during Mesozoic oceanic anoxic events. J. Geol. Soc. 161, 353–364.
Peters, K.E., Moldowan, J.M., 1991. Effects of Source, Thermal Maturity, and Biodegradation on the Distribution and Isomerization of Homohopanes in Petroleum. Organic Geochem. 17, 47–51. https://doi.org/10.1016/0146-6380(91)90039-M.
Peters, C.C., Walters, C., Moldowan, J.M., 2005. The Biomarker Guide: Volume II. Biomarkers and Isotopes in Petroleum Systems and Earth History. Cambridge University Press.
Piper, D.Z., Calvert, S.E., 2009. A marine biogeochemical perspective on black shale deposition. Earth Sci. Rev. 95, 63–96.
Plint, A.G., 2000. Sequence stratigraphy and palaeogeography of a Cenomanian deltaic complex: the Dunvegan and lower Kaskapau formations in subsurface and outcrop, Alberta and British Columbia, Canada. Bull. Can. Petrol. Geol. 48, 43–79.
Plint, A.G., Macquaker, J.H.S., Varban, B.L., 2012. Bedload transport of mud across a wide, storm-influenced ramp: Cenomanian-Turonian Kaskapau Formation, Western Canada Foreland Basin. J. Sediment. Res. 82, 801–822.
Pratt, L.M., 1985. Isotopic Studies of Organic Matter and Carbonate in Rocks of the Greenhorn Marine Cycle. https://doi.org/10.2110/sepmfg.04.038.
Pratt, L.M., Threlkeld, C.N., 1984. Stratigraphic significance of 13C/12C ratios in mid-Cretaceous rocks of the western interior, U.S.A. In: Mesozoic of Middle North America. Canadian Society Petroleum Geologists, pp. 305–312.
Prauss, M.L., 2007. Availability of reduced nitrogen chemospecies in photic-zone waters as the ultimate cause for fossil prasinophyte prosperity. PALAIOS 22, 489–499.
Riva, A., Caccialanza, P.G., Quagliaroli, F., 1988. Recognition of 18β (H)oleanane in several crudes and Tertiary-Upper Cretaceous sediments. Definition of a new maturity parameter. Organic Geochemistry. In: Proceedings of the 13th International Meeting on Organic Geochemistry 13, pp. 671–675.
Robinson, S.A., Heimhofer, U., Hesselbo, S.P., Petrizzo, M.R., 2017. Mesozoic climates and oceans - a tribute to Hugh Jenkyns and Helmut Weissert. Sedimentology 64, 1–15.
Rizzi, M, Hovikoski, J, Schovsbo, N H, Therkelsen, J, Olivarius, M, Nytoft, H P, Nga, L H, Thuy, N T T, Toan, D M, Bojesen-Koefoed, J, Petersen, H I, Nielsen, L H, Abatzis, I, Korte, C, M, B W Fyhn, 2020. Factors controlling accumulation of organic carbon in a rift-lake, Oligocene Vietnam. Sci. Rep. 10 (1), 14976. https://doi.org/10.1038/s41598-020-71829-7.
Sageman, B.B., 1996. Lowstand tempestites: depositional model for Cretaceous skeletal limestones, Western Interior basin. Geology 24, 888–892.
Sageman, B.B., Meyers, S.R., Arthur, M.A., 2006. Orbital time scale and new C-isotope record for Cenomanian-Turonian boundary stratotype. Geology 34, 125–128.
Savrda, C.E., 1998. Ichnology of the Bridge Creek Limestone: Evidence for Temporal and Spatial Variations in Palaeo-Oxygenation in the Western Interior Seaway. https://doi.org/10.2110/csp.98.06.0127.
Schlanger, S.O., Arthur, M.A., Jenkyns, H.C., Scholle, P.A., 1987. The Cenomanian-Turonian Oceanic Anoxic Event, I. Stratigraphy and distribution of organic carbon-rich beds and the Marine delta 13C excursion. Marine petroleum source rocks.
Schlanger, S.O., Jenkyns, H.C., 1976. Cretaceous oceanic anoxic events: causes and consequences. Geol. Mijnb. 55, 179–184.
Schmidtko, S., Stramma, L., Visbeck, M., 2017. Decline in global oceanic oxygen content during the past five decades. Nature 542, 335-+.
Schröder-Adams, C., 2014. The cretaceous Polar and Western Interior seas: palaeoenvironmental history and palaeoceanographic linkages. Sediment. Geol. 301, 26–40.
Schröder-Adams, C.J., Cumbaa, S.L., Bloch, J., Leckie, D.A., Craig, J., El-Dein, S.A.S., Simons, D.J.H.A.E., Kenig, F., 2001. Late Cretaceous (Cenomanian to Campanian) palaeoenvironmental history of the Eastern Canadian margin of the Western Interior Seaway: bonebeds and anoxic events. Palaeogeogr. Palaeoclimatol. Palaeoecol. 170, 261–289.
Schröder-Adams, C.J., Herrle, J.O., Tu, Q., 2012. Albian to Santonian carbon isotope excursions and faunal extinctions in the Canadian Western Interior Sea: recognition of eustatic sea-level controls on a forebulge setting. Sediment. Geol. 281, 50–58.
Schröder-Adams, C.J., Leckie, D.A., Bloch, J., Craig, J., McIntyre, D.J., Adams, P.J., 1996. Palaeoenvironmental changes in the cretaceous (Albian to Turonian) Colorado Group of western Canada: Microfossil, sedimentological and geochemical evidence. Cretac. Res. 17, 311–365.
Schwark, L., Empt, P., 2006. Sterane biomarkers as indicators of palaeozoic algal evolution and extinction events. In: Palaeogeography, Palaeoclimatology, Palaeoecology, Evolution of the System Earth in the Late Palaeozoic: Clues from Sedimentary Geochemistry, 240, pp. 225–236.
Scott, R.W., Franks, P.C., Evetts, M.J., Bergen, J.A., Stein, 1998. Timing of mid-Cretaceous relative sea level changes in the Western Interior: Amoco No. 1 Bounds Core.. In: SEPM Concepts in Sedimentology and Palaeontology 6, pp. 11–34.
Seifert, W.K., Moldowan, J.M., 1981. Paleoreconstruction by biological markers. Geochim. Cosmochim. Acta 45 (6), 783–794.
Simons, D.J.H., Kenig, F., 2001. Molecular fossil constraints on the water column structure of the Cenomanian-Turonian Western Interior Seaway, USA. Palaeogeogr. Palaeoclimatol. Palaeoecol. 169, 129–152.
Simons, D.J.H., Kenig, F., Schroder-Adams, C.J., 2003. An organic geochemical study of Cenomanian-Turonian sediments from the Western Interior Seaway, Canada. Org. Geochem. 34, 1177–1198.
Sinninghe Damsté, J.S., Kenig, F., Koopmans, M.P., Köster, J., Schouten, S., Hayes, J.M., de Leeuw, J.W., 1995. Evidence for gammacerane as an indicator of water column stratification. Geochim. Cosmochim. Acta 59, 1895–1900.
Slingerland, R., Kump, L.R., Arthur, M.A., Fawcett, P.J., Sageman, B.B., Barron, E.J., 1996. Estuarine circulation in the Turonian Western Interior seaway of North America. Geol. Soc. Am. Bull. 108, 941–952.
Sun, X., Zhang, T., Sun, Y., Milliken, K.L., Sun, D., 2016. Geochemical evidence of organic matter source input and depositional environments in the lower and upper Eagle Ford Formation, South Texas. Org. Geochem. 98, 66–81.
Takashima, R., Nishi, H., Huber, B., Leckie, R.M., 2006. Greenhouse World and the Mesozoic Ocean. Oceanography 19, 82–92.
Tappan, H., 1980. Palaeobiology of Plant Protists. W.H.Freeman & Co Ltd, San Francisco.
Ten Haven, H.L., Deleeuw, J.W., Rullkotter, J., Damste, J.S.S., 1987. Restricted utility of the pristane phytane ratio as a palaeoenvironmental indicator. Nature 330, 641–643.
Ten Haven, H.L., Rohmer, M., Rullkotter, J., Bisseret, P., 1989. Tetrahymanol, the most likely precursor of gammacerane, occurs ubiquitously in marine-sediments. Geochim. Cosmochim. Acta 53, 3073–3079.
Tissot, B.P., Welte, D.H., 1984. Production and accumulation of organic matter: The organic carbon cycle. In: Petroleum Formation and Occurrence, pp. 3–13.
Trabucho Alexandre, J., Tuenter, E., Henstra, G.A., van der Zwan, van de Wal, Dijkstra, H.A., de Boer, 2010. The mid-Cretaceous North Atlantic nutrient trap: black shales and OAEs. Paleoceanography. 25 (4), PA4201.
Tsikos, H., Jenkyns, H.C., Walsworth-Bell, B., Petrizzo, M.R., Forster, A., Kolonic, S., Erba, E., Silva, I.P., Baas, M., Wagner, T., Damste, J.S.S., 2004. Carbon-isotope stratigraphy recorded by the Cenomanian-Turonian Oceanic Anoxic Event: correlation and implications based on three key localities. J. Geol. Soc. 161, 711–719.
Turgeon, S.C., Creaser, R.A., 2008. Cretaceous oceanic anoxic event 2 triggered by a massive magmatic episode. Nature 454, 323–326.
Tyson, R., 1995. Sedimentary Organic Matter: Organic Facies and Palynofacies. Springer, Netherlands. https://doi.org/10.1007/978-94-011-0739-6.
Upchurch, G.R., Wolfe, J.A., 1993. Cretaceous vegetation of the western interior and adjacent regions of North America, evolution of the Western Interior Basin. Geol. Assoc. Can. Spec. Pap. 243–281.
van de Schootbrugge, B., Bailey, T.R., Rosenthal, Y., Katz, M.E., Wright, J.D., Miller, K. G., Feist-Burkhardt, S., Falkowski, P.G., 2005. Early Jurassic climate change and the radiation of organic-walled phytoplankton in the Tethys Ocean. Palaeobiology 31, 73–97.
van Helmond, N.A.G.M., Sluijs, A., Papadomanolaki, N.M., Plint, A.G., Grocke, D.R., Pearce, M.A., Eldrett, J.S., Trabucho-Alexandre, J., Walaszczyk, I., van de Schootbrugge, B., Brinkhuis, H., 2016. Equatorward phytoplankton migration during a cold spell within the late cretaceous super-greenhouse. Biogeosciences 13, 2859–2872.
van Helmond, N.A.G.M., Sluijs, A., Reichart, G.-J., Damsté, J.S.S., Slomp, C.P., Brinkhuis, H., 2014. A perturbed hydrological cycle during Oceanic Anoxic Event 2. Geology 42, 123–126.
Varban, B.L., Plint, A.G., 2008. Palaeoenvironments, palaeogeography, and physiography of a large, shallow, muddy ramp: Late Cenomanian-Turonian Kaskapau Formation, Western Canada foreland basin. Sedimentology 55, 201–233.
Vizcaíno, M., Yurchenko, I., Forkner, R., Fildani, A., Owens, J., Duncan, L., Sperling, E., 2020. In: Meta-Analysis Identifies Global and Regional Change during Cretaceous Ocean Anoxic Event 2. Presented at the Goldschmidt2020, p. 2689.
Volkman, J.K., 1986. A review of sterol markers for marine and terrigenous organic matter. Org. Geochem. 9 (2), 83–99.
Volkman, J., 2003. Sterols in microorganisms. Appl. Microbiol. Biotechnol. 60, 495–506.
Volkman, J.K., Barrett, S.M., Dunstan, G.A., Jeffrey, S.W., 1994. Sterol biomarkers for microalgae from the green algal class Prasinophyceae. Org. Geochem. 21, 1211–1218.
Volkman, J.K., Barrett, S.M., Blackburn, S.I., Mansour, M.P., Sikes, E.L., Gelin, F., 1998. Microalgal biomarkers: a review of recent research developments. Org. Geochem. 29, 1163–1179. https://doi.org/10.1016/S0146-6380(98)00062-X.
Wang, J., Jacobson, A.D., Sageman, B.B., Hurtgen, M.T., 2021. Stable Ca and Sr isotopes support volcanically triggered biocalcification crisis during Oceanic Anoxic Event 1a. Geology 49 (5), 515–519.
Wells, M.L., Trainer, V.L., Smayda, T.J., Karlson, B.S.O., Trick, C.G., Kudela, R.M., Ishikawa, A., Bernard, S., Wulff, A., Anderson, D.M., Cochlan, W.P., 2015. Harmful algal blooms and climate change: learning from the past and present to forecast the future. Harmful Algae 49, 68–93.
West, O.L.O., Leckie, R.M., Schmidt, M., 1998. Foraminiferal Palaeoecology and Palaeoceanography of the Greenhorn Cycle Along the Southwestern Margin of the Western Interior Sea. https://doi.org/10.2110/csp.98.06.0079.
White, T., Arthur, M.A., 2006. Organic carbon production and preservation in response to sea-level changes in the Turonian Carlile Formation, U.S. Western Interior Basin.

Palaeogeography, Palaeoclimatology, Palaeoecology, Causes and Consequence of Marine Organic Carbon Burial Through Time 235, 223–244.
YIn, J., Hao, F., Wang, Z., Chen, X., Zou, H., 2020. Lacustrine conditions control on the distribution of organic-rich source rocks: An instance analysis of the lower 1st member of the Shahejie Formation in the Raoyang Sag, Bohai Bay Basin. J. Nat. Gas Sci. Eng. 78 https://doi.org/10.1016/j.jngse.2020.103320.
Zeng, Z., Pike, M., Tice, M.M., Kelly, C., Marcantonio, F., Xu, G., Maulana, I., 2018. Iron fertilization of primary productivity by volcanic ash in the Late Cretaceous (Cenomanian) Western Interior Seaway. Geology 46, 859–862.